Published in final edited form as:

Neuron. 2015 May 20; 86(4): 971–984. doi:10.1016/j.neuron.2015.03.064.

Functional Assembly of Accessory Optic System Circuitry Critical for Compensatory Eye Movements

Lu O. Sun[1,5], **Colleen M. Brady**[1,6], **Hugh Cahill**[2,7], **Timour Al-Khindi**[1], **Hiraki Sakuta**[3], **Onkar S. Dhande**[4], **Masaharu Noda**[3], **Andrew D. Huberman**[4], **Jeremy Nathans**[2], and **Alex L. Kolodkin**[1]

[1]The Solomon H. Snyder Department of Neuroscience, Howard Hughes Medical Institute, The Johns Hopkins University School of Medicine, Baltimore, MD 21205, USA.

[2]Department of Molecular Biology and Genetics, Department of Neuroscience, Department of Ophthalmology, Howard Hughes Medical Institute, The Johns Hopkins University School of Medicine, Baltimore, MD 21205, USA.

[3]Division of Molecular Neuroscience, National Institute for Basic Biology, 5-1 Higashiyama, Myodaiji-cho, Okazaki 444-8787, Japan.

[4]Department of Neurosciences, Neurobiology Section in the Division of Biological Sciences, Department of Ophthalmology, University of California, San Diego, CA 92093, USA.

SUMMARY

Accurate motion detection requires neural circuitry that compensates for global visual field motion. Select subtypes of retinal ganglion cells perceive image motion and connect to the accessory optic system (AOS) in the brain, which generates compensatory eye movements that stabilize images during slow visual field motion. Here, we show that the murine transmembrane semaphorin 6A (Sema6A) is expressed in a subset of On direction-selective ganglion cells (On DSGCs) and is required for retinorecipient axonal targeting to the medial terminal nucleus (MTN) of the AOS. Plexin A2 and A4, two Sema6A binding partners, are expressed in MTN cells, attract $Sema6A^+$ On DSGC axons, and mediate MTN targeting of $Sema6A^+$ RGC projections. Furthermore, Sema6A/Plexin-A2/A4 signaling is required for the functional output of the AOS. These data reveal molecular mechanisms underlying the assembly of AOS circuits critical for moving image perception.

Corresponding Author: Alex L. Kolodkin <kolodkin@jhmi.edu>.

[5]Present address: Department of Neurobiology, Stanford University School of Medicine, 299 Campus Drive, Stanford, CA 94305, USA.

[6]Present address: Baylor College of Medicine, One Baylor Plaza, Houston, TX 77030, USA.

[7]Present address: Joan C. Edwards School of Medicine at Marshall University, 1600 Medical Center Drive, Huntington, WV 25701, USA.

INTRODUCTION

The detection of object motion is an essential visual system function mediated by direction selective (DS) circuitry in the retina and in retinorecipient brain regions targeted by DS retinal ganglion cells (RGCs). In addition to tracking moving objects, a critical function served by visual system DS responses is the ability to compensate for global visual field motion. This can be caused by the observer's rapid head movements, or by overall slow movement of the observer through the visual scene. Failure to execute image-stabilizing eye movements that compensate for self-induced global visual field motion results in blurred image perception. To prevent this, the accessory optic system (AOS) of the mammalian visual system and the vestibular system converge to direct oculomotor output critical for image stabilization (Simpson, 1984). The vestibular semicircular canals compensate for rapid head movements by driving eye rotation in the opposite direction to generate the vestibular ocular reflex (VOR). The AOS, responding to slow velocity motion of the visual field, elicits finely graded eye movements called the optokinetic reflex (OKR) that compensate for retinal slip and stabilize slowly moving images (Masseck and Hoffmann, 2009). The AOS constitutes the primary visual system motion circuitry present in all vertebrates, including humans (Fredericks et al., 1988; Kubo et al., 2014; Masseck and Hoffmann, 2009; Simpson, 1984), and it includes subpopulations of direction-selective ganglion cells (DSGCs) and their central targets in the midbrain. In mice, these central targets are the medial terminal nucleus (MTN) in the ventral region of midbrain adjacent to the cerebral peduncle and substantia nigra, and the dorsal terminal nucleus (DTN) and the nucleus of the optic tract (NOT), which together are located in the dorsal midbrain anterior to the superior colliculus (SC) (Dhande and Huberman, 2014).

Although AOS anatomy was described over a century ago (reviewed in: (Simpson, 1984)), the recent development of genetic tools has aided in the identification and functional analysis of its various components (Dhande et al., 2013; Kay et al., 2011; Triplett et al., 2014; Yonehara et al., 2009; Yonehara et al., 2008). AOS brain targets receive direct retinal input from both On direction-selective ganglion cells (On DSGCs) and also from a subpopulation of On-Off DSGCs. On DSGCs, which respond to bright objects moving at slow speed, are a major retinal AOS component. The dendrites of On DSGCs co-stratify with On starburst amacrine cell (On SAC) dendrites in the S4 sublamina of the retina. On DSGC axons project to all three AOS nuclei in the midbrain: the MTN, DTN, and NOT (Dhande et al., 2013; Yonehara et al., 2009; Yonehara et al., 2008). In addition to On DSGCs, a newly discovered population of On-Off DSGCs with relatively small dendritic fields and a preference for forward, slow-velocity, image motion target the NOT and SC (Dhande et al., 2013). DSGC innervation of the different AOS brain targets mediates distinct OKR responses; innervation of the MTN drives vertical OKRs, whereas innervation of the DTN/NOT mediates horizontal OKRs (Fredericks et al., 1988; Pak et al., 1987; Simpson, 1984).

Mammalian RGCs establish connections with central brain targets during embryonic and early postnatal development (Haupt and Huber, 2008). The assembly of visual system circuits depends upon a series of accurately executed events during neural development, including: emergence and extension of RGC axons within the developing retina towards the

inner limiting membrane (ILM); outgrowth and guidance of RGC axons out of the retina through the optic nerve head; segregation of ipsilateral and contralateral RGC axon projections at the optic chiasm; initial targeting of axons to various retinorecipient brain regions; elaboration of synapses; and pruning and refinement of RGC projections (Sanes and Zipursky, 2010). A myriad of molecules and signaling pathways direct these events during the assembly of the vertebrate main optic system, including retinorecipient targeting and RGC projection refinement (Haupt and Huber, 2008). For example, ephrins, Wnts and their receptors are required for topographic mapping of RGC axons within the superior colliculus (SC) (McLaughlin and O'Leary, 2005; Schmitt et al., 2006), and Eph receptor-dependent and independent signaling pathways direct retinogeniculate targeting (Culican et al., 2009; Nie et al., 2010). In zebrafish, slit-Robo signaling along with extracellular matrix components sculpt laminae-specific targeting of RGC axons within the tectum (Robles and Baier, 2012). However, the mechanisms underlying retinorecipient targeting to specific areas of the AOS remain unknown.

Here, we identify a guidance cue signaling pathway that is essential for retinorecipient targeting during AOS development. We show that plexin A2 (PlexA2)/PlexA4-semaphorin 6A (Sema6A) signaling regulates On DSGC innervation of the MTN, utilizing "reverse signaling" whereby Sema6A functions as a receptor in RGC axons. The failure of On DSGCs to innervate the MTN in the absence of PlexA2/PlexA4-Sema6A signaling leads to specific OKR defects. These results provide insight into how DSGCs establish connectivity with their retinorecipient targets to support AOS visual behaviors.

RESULTS

Sema6A is Expressed in On DSGCs but not *TRHR-GFP*$^+$ or *DRD4-GFP*$^+$ On-Off DSGCs

The transmembrane semaphorin Sema6A is expressed in On SACs and is required for certain direction selective (DS) responses to fast moving objects in On-Off DSGCs (Sun et al., 2013). Our analysis of Sema6A expression also revealed that it is expressed in a subset of RGCs (Matsuoka et al., 2011b). To determine whether Sema6A might play additional roles in the perception of image motion, we identified the type(s) of RGCs that express Sema6A. By examining co-expression of Sema6A and GFP in wholemount retinas from transgenic lines that express GFP in specific subtypes of RGCs, we found that Sema6A is expressed in all GFP$^+$ On DSGCs labeled in the ventral retina of the *SPIG1::GFP* knock-in mouse line (Yonehara et al., 2009; Yonehara et al., 2008) (Figures 1A–A" and Figures S1A–D"). These On DSGCs have dendrites that stratify together with On SACs in the inner plexiform layer (IPL) of the retina, and they respond to relatively slow-velocity vertical image motion (Yonehara et al., 2009). Furthermore, their axons project to the medial terminal nucleus (MTN), a central AOS retinorecipient target. SPIG1::GFP$^+$ RGCs are Sema6A immunopositive throughout early postnatal retina development (Figures S1A–D" and S1E–H"; quantified in Figure 1I). In addition, Sema6A immunoreactivity is detected in most Hoxd10-GFP$^+$ RGCs (Figures 1B–B", quantified in Figure 1I) in retinas from a BAC transgenic line (*Hoxd10-GFP*) in which GFP is expressed in all three populations of AOS On DSGCs: On DSGCs that respond to lower-velocity upward, downward, or forward motion, and also a small population of AOS On-Off DSGCs that responds to forward lower-

velocity image motion (Dhande et al., 2013). Thus, RGCs that project to AOS structures in the brain express Sema6A.

To further investigate Sema6A protein distribution, we performed ocular injections of cholera toxin subunit b conjugated with Alexa555 (CTB-555) to label RGC axon projections, including those to the MTN (the major retinorecipient target of On DSGCs tuned to slow motion detection along the dorsal-ventral axis (Yonehara et al., 2008)), followed by Sema6A immunohistochemistry. We found that Sema6A immunoreactivity co-localizes with CTB-555 fluorescence (Figures 1C–C"). We also utilized an alkaline phosphatase (AP) colorimetric reaction in the *Sema6A* heterozygous mouse line that harbors a "PLAP Trap" insertion in a *Sema6A* intron, and thus expresses AP robustly in axons extending from Sema6A^{+} neurons (Leighton et al., 2001), to identify RGC axon projections that are Sema6A^{+}. We found that the AP reaction product is present in axons that include those which innervate the MTN (Figures 1D–D"', white arrows). These results show that Sema6A is expressed in On DSGCs and strongly suggest that Sema6A protein is present in both cell bodies and axons of On DSGCs that innervate the MTN.

A second major population of direction-selective ganglion cells, On-Off DSGCs, stratify their dendrites with both On and Off SACs in the IPL, project their axons to the dorsal lateral geniculate nucleus (dLGN) of the thalamus and the SC in the dorsal midbrain, and includes RGCs that respond to higher-velocity image motion in all four cardinal directions (Dhande and Huberman, 2014). Is Sema6A expressed in these On-Off DSGCs? We performed wholemount Sema6A immunohistochemistry on retinas derived from *DRD4-GFP* and *TRHR-GFP* mice, two well-characterized BAC transgenic lines that genetically label subpopulations of On-Off DSGCs (Huberman et al., 2009; Kay et al., 2011; Rivlin-Etzion et al., 2011). Sema6A immunoreactivity is not detected in DRD4-GFP^{+} (Figures 1E–E" and S1I–L") and is observed in only a very small fraction of postnatal day 1 (P1) TRHR-GFP^{+} (Figures 1F–F" and S1M–P") RGC cell bodies (quantified in Figure 1I). In addition, *Sema6A*$^{AP+}$ fibers are not present in the outer shell of the dLGN (Figures 1G–G") or the superficial layer of the SC (Figures 1H–H"), two well-characterized On-Off DSGC retinorecipient targets (Rivlin-Etzion et al., 2011), in mice heterozygous for the PLAP-Trap *Sema6A* allele. Moreover, we found that at P10 Sema6A immunoreactivity does not colocalize with cocaine- and amphetamine- regulated transcript (CART) (Figures S1Q–Q"), a marker for the vast majority of On-Off DSGCs but not for Hoxd10-GFP^{+} On-Off DSGCs (Dhande et al., 2013; Kay et al., 2011). Therefore, Sema6A is a marker of AOS RGCs but is not expressed by On-Off DSGCs involved in image formation.

Sema6A is Required for the Development of Accessory Optic System Trajectories

The selective expression of Sema6A in cell bodies and axons of On DSGCs raised the possibility that Sema6A directly participates in the development of these neurons. We first analyzed the central projections of On DSGCs in wild-type and *Sema6A*$^{-/-}$ null mutants using ocular CTB injections. In wild-type adult mice innervation of the MTN, a major On DSGC central target, can be visualized on the ventral brain surface in whole-mount preparations (white arrows in Figure 2A) and also in coronal brain sections (white arrow in Figure 2B). Axon projections to the MTN in *Sema6A*$^{-/-}$ mutants are greatly diminished

(Figures 2A' and 2B'). Although there is residual innervation of the dorsal-most and ventral-most regions of the MTN, axon projections to most of the MTN are absent in *Sema6A*$^{-/-}$ mutants (n=13 animals, phenotype observed with complete penetrance and expressivity). To further investigate On DSGC-MTN innervation we used two mouse lines that genetically label On DSGCs: *SPIG1::GFP*, which labels a subset of MTN-innervating On DSGCs from embryonic stage e12.5 to postnatal developmental stages up to ~P13 (Yonehara et al., 2009; Yonehara et al., 2008), when the GFP signal becomes very weak; and *Hoxd10-GFP*, which labels all On DSGCs from late embryonic stages through adulthood (Dhande et al., 2013; Osterhout et al., 2014). We observed GFP expression following introduction of these GFP alleles into *Sema6A*$^{-/-}$ mutants and found that both SPIG1::GFP^{+} (Figures 2C–D') and Hoxd10-GFP^{+} (Figures S2A–B') projections that innervate the MTN are greatly diminished in *Sema6A*$^{-/-}$ mutants, providing additional support for the conclusion that Sema6A is required for On DSGC connectivity with the MTN.

In addition to the MTN, AOS On DSGCs also innervate two additional midbrain targets: the dorsal terminal nucleus (DTN) and the nucleus of optic tract (NOT) (Simpson, 1984). To characterize On DSGC axonal innervation of these AOS retinorecipient targets, we performed ocular CTB injections and genetic labeling experiments in control and *Sema6A*$^{-/-}$ mutants. Compared to the controls, *Sema6A*$^{-/-}$ On DSGC axonal projections to the DTN are reduced but still present (Figures 2E and 2E', Figures S2G and S2G'), whereas innervation of the NOT is unaffected (Figures 2F, 2F', S2H and S2H'). Thus, Sema6A is partially required for On DSGC-DTN innervation but is apparently dispensable for projections to the NOT.

Is Sema6A required for retinorecipient targeting by other classes of RGCs? We first utilized ocular CTB injections to assess general RGC targeting in control and *Sema6A*$^{-/-}$ mutants. Compared to wild-type, *Sema6A*$^{-/-}$ mutants exhibit normal RGC innervation of the LGN (Figures S2C and S2C'), SC (Figures S2D and S2D'), suprachiasmatic nucleus (SCN) (Figures S2E and S2E'), and olivery pretectal nucleus (OPN) (Figures S2F and S2F'). We next characterized the axonal projections of Sema6A immunonegative On-Off DSGCs in *Sema6A*$^{-/-}$ mutants. We crossed the *TRHR-GFP* and *DRD4-GFP* reporter alleles into *Sema6A*$^{+/-}$ and *Sema6A*$^{-/-}$ backgrounds, genetically labeling the central projections of these two types of On-Off DSGC. In *Sema6A*$^{+/-}$ mice, both TRHR-GFP^{+} and DRD4-GFP^{+} axons target the "shell" region of the dLGN (Figures 2G and S2I) and the superficial layer of the SC (Figures 2H and S2M) (see also (Rivlin-Etzion et al., 2011)). In *Sema6A*$^{-/-}$ mutants, both TRHR-GFP^{+} and DRD4-GFP^{+} On-Off DSGCs exhibit normal dLGN (Figures 2G' and S2I') and SC (Figures 2H' and S2M') innervation, showing that Sema6A is not required for retinorecipient targeting by these On-Off DSGCs. In addition, analysis of other RGC subtypes revealed no obvious defects with respect to retinorecipient targeting to the dLGN "core" (revealed by *CB2-GFP* (Huberman et al., 2008b), Figures S2J and S2J'); IGL and vLGN (revealed by *Cdh3-GFP* (Osterhout et al., 2011), Figures S2K and S2K'); and OPN (revealed by *Cdh3-GFP* (Osterhout et al., 2011), Figures S2L and S2L') in *Sema6A*$^{-/-}$ mutants. Therefore, Sema6A is required specifically for the innervation of a subset of AOS targets in the brain.

Retinorecipient targeting proceeds in multiple steps, including initial targeting by early-arriving RGC axons, subsequent innervation by follower axons, and pruning to remove excess projections (Haupt and Huber, 2008; Huberman et al., 2008a). In which phase does Sema6A act to pattern On DSGC axonal innervation? We addressed this question by analyzing the innervation pattern of SPIG1::GFP$^+$ RGC axons throughout embryonic and early postnatal visual system development. In control animals, SPIG1::GFP$^+$ axon are observed at their ventral midbrain target at e14.5 (Figure 3A). Additional SPIG1::GFP$^+$ axons reach the MTN at e16.5 (Figure 3B), and MTN innervation by RGCs becomes apparent throughout late embryonic development (Figures 3C and 3D) (Yonehara et al., 2008). In *Sema6A*$^{-/-}$ mutants, SPIG1::GFP$^+$ fibers reach their target at e14.5 (Figure 3A'), similar to what we observe in *Sema6A*$^{+/-}$ controls: both normalized fiber intensity (a measure of total innervation of the MTN region, see Supplemental Experimental Procedures), and total innervation area (see Supplemental Experimental Procedures) were not significantly different (Figures 3E and S3C). However, at e16.5, *Sema6A*$^{-/-}$; *SPIG1::GFP*$^+$ fibers appear defasciculated and innervate a much broader area in the region of the MTN compared to controls (red arrows in Figure 3B', quantified in Figure S3C). Interestingly, the normalized fiber intensities at e16.5 are the same in *Sema6A*$^{-/-}$ mutants and controls (quantified in Figure 3E), suggesting that RGC axons innervating the MTN do not retract or degenerate at this early developmental stage. These innervation defects become more severe at later developmental stages, as reflected by the significant reduction in the intensity of GFP expression over the MTN region as development proceeds (Figures 3C' (e18.5) and 3D' (P1); quantification in Figures 3E and S3C). Thus, On DSGC axons reach the MTN in *Sema6A*$^{-/-}$ mutants during early embryonic stages, but mutant On DSGC axons innervate the MTN in a defasciculated fashion rather than as a discrete bundle and extend over a wide region in the vicinity of the MTN. By e18.5, reduced innervation in *Sema6A*$^{-/-}$ mutants is apparent in the ventral MTN region. This reduction in innervation continues as development proceeds and is quite robust by P1 (Figures 3A–D', quantified in Figure 3E).

The On DSGC-MTN innervation defects observed in *Sema6A*$^{-/-}$ mutants raise the critical issue of whether On DSGC cell number is altered in these mutants. To address this question, we used the *SPIG1::GFP* allele to label On DSGC cell bodies throughout retina development. *Sema6A*$^{-/-}$; *SPIG1::GFP*$^+$ RGC cell number is the same as what we observe in *Sema6A*$^{+/-}$; *SPIG1::GFP*$^+$ RGCs at e14.5 (Figures 3F, 3F', S3F and S3F"). Importantly, loss of Sema6A does not affect SPIG1::GFP$^+$ cell numbers at later embryonic stages, when the On DSGC-MTN innervation defects in *Sema6A*$^{-/-}$ mutants are already prominent (at e16.5: Figures 3G, 3G', S3G and S3G'; and at e18.5: Figures 3H, 3H', S3H and S3H'). RGC apoptosis during retinal development is normally apparent by e18.5 (Pequignot et al., 2003), and this is reflected in the reduction of GFP$^+$ On DSGCs we observe in *SPIG1::GFP; Sema6A*$^{+/-}$ retinas from late embryogenesis to P10 (Figures 3F–I and S3F–K, quantified in Figure 3J). However, we observe in *SPIG1::GFP; Sema6A*$^{-/-}$ retinas that GFP$^+$ RGC cell number exhibits a greater decrease than in controls, starting at P1 and continuing throughout early postnatal retina development (Figures 3F'-I' and S3F'-K', quantified in Figure 3J). By P10, *SPIG1::GFP; Sema6A*$^{-/-}$ retinas exhibit 68% of the number of GFP$^+$ RGCs observed in *SPIG1::GFP; Sema6A*$^{+/-}$ retinas (control GFP$^+$ cell

number in the ventral retina=304.7±9.4, *Sema6A*$^{-/-}$ GFP^{+} cell number in the ventral retina=95.8±7.1; mean±SEM, P <10−^{6}). Cell apoptosis analysis also reveals a significant increase in *SPIG1::GFP; Sema6A*$^{-/-}$ retinas at e18.5 as compared to controls with respect to RGCs that are immuno-positive for both SPIG1::GFP and Cleaved-Caspase3 (Figures S4G–I', quantified in Figure S4J); this shows that an increased number *of Sema6A*$^{-/-}$*; SPIG1::GFP*$^{+}$ RGCs undergo cell apoptosis during late embryogenesis compared to apoptosis normally observed at this stage in *Sema6A*$^{+/-}$*; SPIG1::GFP*$^{+}$ retinas. Therefore, Sema6A^{+} On DSGC axons project to, and elaborate within, the MTN region during embryonic development. In the absence of *Sema6A*, On DSGCs exhibit aberrant MTN innervation that is apparent at e16.5 and at e18.5, developmental time points when On DSGC cell number in this mutant remains similar to controls. However, by P1 MTN innervation defects become apparent, as does enhanced On DSGC apoptosis.

To determine whether the reduction in GFP^{+} RGCs in *Sema6A*$^{-/-}$ mutants is not particular to *SPIG1::GFP* reporter mice, we also characterized GFP^{+} RGC number using the *Hoxd10-GFP* reporter in *Sema6A*$^{+/-}$ and *Sema6A*$^{-/-}$ genetic backgrounds. An advantage of using *Hoxd10-GFP* is that in this line GFP expression persists throughout adulthood (Dhande et al., 2013; Osterhout et al., 2014), unlike the *SPIG1::GFP* reporter in which GFP expression diminishes in the ventral retina during postnatal development and ceases by P13 (Yonehara et al., 2008). Compared to control retinas, *Sema6A*$^{-/-}$*; Hoxd10-GFP*$^{+}$ RGC number exhibits a significant decrease of ~37% in retinas of 3 week-old animals (compare Figures 3K and 3K'; quantified in Figure 3L; *Sema6A*$^{+/-}$*; Hoxd10-GFP*$^{+}$ cell density=189.6±5.8/mm^{2}, and *Sema6A*$^{-/-}$*; Hoxd10-GFP*$^{+}$ cell density=118.9±7.0/mm^{2}; mean±SEM, P<10^{-5}). The decrease in GFP^{+} RGC number in P21 *Hoxd10-GFP; Sema6A*$^{-/-}$ mutants is much less than that observed in P10 *SPIG1::GFP; Sema6A*$^{-/-}$ mutants (~37% compared to ~68%, respectively), and this likely reflects differences in AOS RGC populations labeled by these two reporters. *SPIG1::GFP* labeling includes On DSGCs in the ventral retina tuned for upward-directed motion (Yonehara et al., 2009), whereas *Hoxd10-GFP* labels On DSGCs tuned for upward, downward, and forward-directed motion, in addition to a newly defined population of forward motion-tuned On-Off DSGCs (Dhande et al., 2013). *Sema6A*$^{-/-}$ mutants show retinorecipient connectivity defects that most strongly compromise MTN innervation, suggesting that Sema6A is required in only a subset of the AOS RGCs labeled by the *Hoxd10-GFP* reporter. Indeed, increased RGC apoptosis observed in *Hoxd10-GFP; Sema6A*$^{-/-}$ retinas compared to controls can be accounted for by loss of a significant fraction of the On DSGCs tuned for vertical motion detection and that innervate the MTN, with the concomitant retention of the other classes of AOS RGCs. Our results strongly suggest that the early *Sema6A*$^{-/-}$ On DSGC-MTN innervation phenotypes contribute to the later increased apoptosis of these DSGCs.

Sema6A is expressed in On SACs (Sun et al., 2013) but not in TRHR-GFP^{+}, DRD4-GFP^{+}, or CART^{+} On-Off DSGCs (Figures 1 and S1). Loss of *Sema6A* does not lead to a change in On SAC cell number, as revealed by anti-ChAT flatmount retinal staining in *Sema6A*$^{-/-}$ mutants and controls (Figures S3D and S3D', quantified in Figure S3E). Further, we find that the number of Brn3b^{+} RGCs (Brn3b^{+} RGCs constitute ~80% of total RGCs (Badea et al., 2009)) is the same in controls and *Sema6A*$^{-/-}$ mutants at P3 (Figures S4K–L),

suggesting that loss of *Sema6A* only affects a subset of On DSGCs (~1% of total RGCs (Yonehara et al., 2008)). As expected, RGC subtypes that do not express Sema6A, including TRHR-GFP^{+} and DRD4-GFP^{+} (Figure 1), show no evidence of increased cell loss in *Sema6A*$^{-/}$ mutants (Figures S4A–E', quantified in Figure S4F). Therefore, Sema6A is not generally required in retinal neurons for cell survival.

PlexA2 and PlexA4 Together Mediate Sema6A-dependent On DSGC-MTN Innervation Through Reverse Signaling

In the absence of Sema6A, On DSGCs arrive in the vicinity of the MTN but extend more broadly in the region of the MTN such that normal target recognition fails, which leads to the subsequent death of a large fraction of these On DSGCs. What are the molecular mechanisms utilized by Sema6A to direct On DSGC-MTN innervation?

PlexA2 serves as a functional Sema6A receptor in several neural tissues including the hippocampus, the cerebellum, and the retina (Renaud et al., 2008; Sun et al., 2013; Suto et al., 2007). For example, *PlexA2*$^{-/-}$ mutants phenocopy *Sema6A*$^{-/-}$ mutants with respect to deficits in dendritic development of On SACs, a cell type that provides presynaptic inhibitory input onto On DSGCs (Sun et al., 2013). PlexA4, along with PlexA2, is also a functional Sema6A receptor in the hippocampus, in subcortical projections to the spinal cord, and in the retina (Matsuoka et al., 2011b; Runker et al., 2008; Suto et al., 2007). In addition, PlexA2 and PlexA4 receptors together mediate Sema6A/6B-dependent development of hippocampal mossy fibers (Suto et al., 2007; Tawarayama et al., 2010). However neither PlexA2 nor PlexA4 is expressed in retinal ganglion cells (Matsuoka et al., 2011a).

We asked if PlexA2 and/or PlexA4 are expressed in the MTN such that they could direct On DSGC-MTN connectivity during AOS development. We utilized a *PlexA2* reporter line in which Cre-dependent recombination results in expression of LacZ under the control of the endogenous *PlexA2* promoter (Sun et al., 2013). Following germline Cre (Sox2-Cre)-dependent recombination we observed X-gal staining in cells residing in the ventral region of the MTN (Figures 4A–B'; see black arrowheads in Figures 4A and 4B). This putative PlexA2 expression pattern was confirmed by performing double immunohistochemistry in the MTN region using antibodies specific for PlexA2 (Suto et al., 2007) and GFP on *SPIG1::GFP* embryonic brain sections (Figures 4C–C"). We found that PlexA2 protein is localized in the ventral MTN (vMTN) region at e18.5, and in addition, robust PlexA4 immunoreactivity is also found in the vMTN region at e18.5 (Figures 4D–D"); the specificity of both antibodies has been previously demonstrated in mutant brains (Suto et al., 2007) and retinas (Matsuoka et al., 2011a; Matsuoka et al., 2011b). We also observed that neither PlexA2 nor PlexA4 immunoreactivity in the vMTN apparently co-localizes with the *SPIG1::GFP* reporter signal in On DSGC axons (insets in Figures 4C–C" and 4D–D"), supporting our previous observation that these plexins are not expressed in RGCs (Matsuoka et al., 2011a). Taken together, these results suggest a "reverse signaling" scenario whereby target-derived PlexA2 and A4 together serve as ligands for Sema6A expressed on On DSGC axons. In this model, transmembrane Sema6A, which has a cytoplasmic domain, functions as a receptor.

To ask whether PlexA2 or PlexA4 regulates Sema6A^{+} On DSGC retinorecipient targeting, we analyzed On DSGC-MTN innervation in *PlexA2*$^{-/-}$ and *PlexA4*$^{-/-}$ single mutants. We found that *PlexA2*$^{-/-}$ mutants exhibit normal development of On DSGC-MTN trajectories, as revealed by CTB ocular injections (Figures 4E and 4F) and also by genetic labeling using *SPIG1::GFP* reporter mice (Figures 4G and 4H). In addition, we found that RGC projections to all other retinorecipient brain targets are generally normal in *PlexA2*$^{-/-}$ mutants (Figures S5A–E' and S5G-K'). Furthermore, all AOS RGC axon trajectories are apparently formed normally in *PlexA4*$^{-/-}$ mutants (Figures 4I-4L), as are most other retinorecipient connections (Figures S6A–B'), consistent with our previous findings (Matsuoka et al., 2011b). These results show that neither PlexA2 nor PlexA4 alone mediates Sema6A-dependent On DSGC-MTN innervation.

To address whether PlexA2 and A4 act redundantly to direct On DSGC innervation of the MTN, we generated *PlexA2*$^{-/-}$*;PlexA4*$^{-/-}$ double mutant mice. *PlexA2*$^{-/-}$*;PlexA4*$^{-/-}$ mice are viable and fertile, and ocular CTB injections reveal that these double mutants exhibit compromised MTN targeting, as seen in wholemount preparations on the ventral brain surface (Figures 5A and 5A') and in coronal brain sections (Figures 5B and 5B'; n=9 animals, and 8/9 show this phenotype), phenocopying *Sema6A*$^{-/-}$ mutants. Interestingly, *PlexA2*$^{-/-}$*;PlexA4*$^{-/-}$ double mutants show completely abrogated DTN innervation (Figures 5C and 5C'; n=9; 8/9 double mutants exhibit this phenotype). This DTN innervation phenotype is much more severe than that observed in *Sema6A*$^{-/-}$ mutants, suggesting that additional cues collaborate with Sema6A to regulate PlexA2/A4-dependent development of On DSGC-DTN trajectories. *PlexA2*$^{-/-}$*;PlexA4*$^{-/-}$ double mutants exhibit generally normal retinorecipient targeting to one additional AOS target (the NOT, Figures 5D and 5D'), image-forming targets (the LGN, Figures 5E and 5E'; the SC, Figures 5F and 5F'), and also non-image-forming retinorecipient targets (the SCN, Figures 5G and 5G'; and the OPN, Figures 5H and 5H'). Importantly, conditional removal of *PlexA2* in the neural retina using *Six3-Cre* (Furuta et al., 2000) in a *PlexA4*$^{-/-}$ background (Matsuoka et al., 2011b; Sun et al., 2013) does not result in any On DSGC-MTN innervation defects (Figures 5I and 5I') or targeting defects to the DTN and NOT (Figures S6C–D'). These results show that these plexins do not function in the retina to mediate retinorecipient targeting of On DSGCs. Other *PlexA* (*PlexA1*$^{-/-}$*;PlexA3*$^{-/-}$ double KO, Figure S6E) and *neuropilin* mutants (Figures S6F–H) exhibit normal On DSGC-MTN innervation, demonstrating that these semaphorin receptors are not required for On DSGC-MTN innervation. Taken together, these results strongly support the idea that Sema6A-PlexA2/A4 "reverse" signaling mediates On DSGC-MTN retinorecipient targeting.

To test whether PlexA2 or A4 can indeed function as ligands to attract Sema6A^{+} On DSGC neurites, we conducted guidance assays using retinal explants grown in culture on alternating "stripes" coated with protein that consists of extracellular plexin domains. We first determined that PlexA2 and PlexA4 ectodomains fused to Fc bind to COS7 cells that express Sema6A (Figures 6A–D' and Figure S7A). We then cultured retinal explants from the ventral region of *SPIG1::GFP; Sema6A*$^{+/+}$ retinas taken at e17.5, a developmental time point when these Sema6A-expressing On DSGCs normally establish connections with the MTN *in vivo* (Yonehara et al., 2008), in dishes coated with recombinant PlexA2 or PlexA4

ectodomain protein presented in stripes. After 2 days *in vitro*, we found that these explants extend GFP^{+} neurites and that these neurites do not exhibit any preference when growing on alternating AP-Fc/BSA stripes (Figures 6E and 6E', and Figure S7B; quantified in Figure 6K). This shows that the AP-Fc control ligand does not attract or repel SPIG1::GFP^{+} neurites. However, when *SPIG1::GFP; Sema6A*$^{+/+}$ explants were grown on plates coated with alternating PlexA2^{Ecto}-Fc/BSA, or PlexA4^{Ecto}-Fc/BSA, recombinant protein stripes (Figures 6F and 6G, respectively), they extend GFP^{+} neurites on the PlexA^{Ecto} stripes (yellow filled arrowheads in Figures 6F and 6G, and also in Figures S7C–D and Figure S7H–M; quantified in Figure 6K), showing that the ectodomains of PlexA2 and PlexA4 can robustly attract SPIG1::GFP^{+} axons. To visualize GFP^{-} neurites, we also stained the explants with antibodies directed against neuron-specific β-III tubulin (TujIII; Figures S7H'-M') (Matsuoka et al., 2011a; Thompson et al., 2006). We found that there are GFP^{-} TujIII^{+} neurites extending from ~1/2 of the retinal explants that do not exhibit preferences for PlexA2^{Ecto} or PlexA4^{Ecto} stripes (yellow open arrowheads in Figures S7H' and S7I', and in Figures S7K' and S7L'; 8/17 explants for PlexA2^{Ecto} stripes, and 12/21 explants for PlexA4^{Ecto} stripes). We also found in ~1/2 of the explants that GFP^{-} TujIII^{+} neurites preferentially grew on PlexA^{Ecto} stripes (red open arrowheads in Figures S7J' and S7M'; 9/17 explants for PlexA2^{Ecto} stripes and 9/21 explants for PlexA4^{Ecto} stripes). Therefore, PlexA2/A4 ectodomain recombinant protein can also attract some SPIG1::GFP^{-} RGC axons extending from these ventral retina explants. This may reflect the ability of SPIG1::GFP^{+} neurites to influence other RGC axons such that they follow along onto PlexA2^{Ecto} stripes, or perhaps the ability of additional RGC populations to be attracted by PlexA^{Ecto} proteins. Taken together, these results show that PlexA2 and PlexA4 ectodomains are sufficient to strongly attract Sema6A^{+} On DSGC axons *in vitro*.

Is PlexA2/A4-induced attraction of SPIG1::GFP^{+} axons mediated by Sema6A? We addressed this point with stripe assays using ventral retina explants derived from *SPIG1::GFP; Sema6A*$^{-/-}$ mice (Figures 6H–J'). Overall, GFP^{+} neurite outgrowth is the same in *SPIG1::GFP; Sema6A*$^{-/-}$ and *SPIG1::GFP; Sema6A*$^{+/+}$ retina explants (Figures S7E–G; quantified in Figure S7N). However, we observed in the absence of Sema6A that axons extending from *SPIG1::GFP; Sema6A*$^{-/-}$ retinal explants were no longer attracted by PlexA2 or PlexA4 ectodomains; GFP^{+} neurites extended freely over PlexA2/A4^{Ecto+} and control stripes (Figures S7E–G, and Figures 6H–J; quantified in Figure 6K), indicating that Sema6A is required in SPIG1::GFP^{+} On DSGC axons to mediate attraction by PlexA2 or PlexA4 ectodomains. In addition, we observed that GFP^{-} TujIII^{+} neurites from *Sema6A*$^{-/-}$ explants do not exhibit preferential growth on PlexA2/A4^{Ecto+} stripes (Figure S7O). Taken altogether, our results strongly suggest that Sema6A functions as a receptor in On DSGCs that signals attraction by PlexA2/A4, thereby guiding On DSGCs to their appropriate AOS target during visual system development.

Sema6A-PlexA2/A4 Signaling Mediates Optokinetic Reflex (OKR) Behavior

On DSGC-MTN connectivity is critical for the normal vertical optokinetic reflex (vOKR) response, whereas On DSGC-DTN/NOT connections drive the horizontal OKR (Masseck and Hoffmann, 2009). We therefore asked whether the specific disruption of AOS retinorecipient targeting in *Sema6A*$^{-/-}$ and *PlexA2*$^{-/-}$*;PlexA4*$^{-/-}$ mutants affects the vOKR

and/or hOKR. In *Sema6A*$^{-/-}$ mutants, in which RGC projections to the DTN are reduced and innervation to the MTN is greatly comprised (Figures 2 and S2), OKR analysis (Cahill and Nathans, 2008) shows that vOKR responses are completely absent (right panel in Figure 7A, quantified in the middle and the right panels of Figure 7B; eye tracking movements (ETMs) per 30 second test interval were 9.11±1.16 for *Sema6A*$^{+/-}$, and 1.06±1.05 for *Sema6A*$^{-/-}$, mean ±S.D.; $P<0.0001$). In contrast, *Sema6A*$^{-/-}$ mutants display a modestly reduced number of hOKR responses (left panel in Figure 7A, quantified in the left and the right panels of Figure 7B; 11.502±1.74 for *Sema6A*$^{+/-}$, and 5.71±2.23 for *Sema6A*$^{-/-}$, mean ±S.D.; $P<0.001$). Therefore, *Sema6A*$^{-/-}$ mutants exhibit a slightly reduced hOKR but virtually no vOKR, in line with the modest defects in DTN targeting and the severe defects in MTN targeting displayed by Sema6A$^{-/-}$ On DSGC axons.

We also determined whether loss of Sema6A affects pupil constriction. Sema6A is not required for RGC projections to the OPN (Figure S2), a nucleus that is important for the pupillary light reflex. Consistent with our anatomical analyses, *Sema6A*$^{-/-}$ mutants have a normal pupillary light reflex (Figure 7C: pupil area (mean ± S.D.) in the dark, 16.81±2.47 mm^2 for *Sema6A*$^{+/-}$, and 14.45±1.75 mm^2 for *Sema6A*$^{-/-}$, $P=0.1368$; in the light, 1.77±0.18 mm^2 for *Sema6A*$^{+/-}$, and 1.53±0.67 mm^2 for *Sema6A*$^{-/-}$, $P=0.5761$). These results show that Sema6A is critical for select visual system responses.

PlexA2$^{-/-}$*; PlexA4*$^{-/-}$ double mutants phenocopy *Sema6A*$^{-/-}$ mutants with respect to On DSGC-MTN innervation, but they also exhibit much more severe On DSGC-DTN targeting phenotypes (Figure 5). To address PlexA2 and A4 involvement in OKR responses, we performed behavioral tests in *PlexA2*$^{+/-}$*;PlexA4*$^{+/-}$, *PlexA2*$^{-/-}$, and *PlexA2*$^{-/-}$*; PlexA4*$^{-/-}$ animals. Compared to *PlexA2*$^{+/-}$*; PlexA4*$^{+/}$- control animals, *PlexA2*$^{-/-}$ mutants exhibit similar vOKRs and hOKRs (Figure 7D, top and middle rows; quantified in Figure 7E), consistent with their normal AOS retinorecipient targeting (Figures 4, Figure 5 and Figure S5) and post-hoc anatomical analyses in these same animals of MTN and DTN innervation (Figures S8A–D and Figure S8I–L). In contrast, *PlexA2*$^{-/-}$*; PlexA4*$^{-/-}$ double mutant mice show significantly diminished horizontal and vertical OKRs (bottom row in Figure 7D, quantified in Figure 7E), and in almost all of these same mice we observe loss of projections to the DTN and the MTN (Figures S8M–P, and S8E–G). In our behavioral tests we observed one *PlexA2*$^{-/-}$*; PlexA4*$^{-/-}$ mouse that still retained a vOKR (mouse #8191, mean vOKR=4.6875 EMT/30s; black arrow in Figure 7E). Our subsequent anatomical analysis revealed that there were limited projections to the MTN in this animal (Figure S8H), supporting a requirement for intact On DSGC-MTN circuitry for this specific AOS function. Taken together, these results show that PlexA2 and PlexA4 act in concert to direct retinorecipient connectivity in the AOS critical for both horizontal and vertical OKR responses.

DISCUSSION

There are over 20 types of RGCs that convey information to discrete brain targets. Little is known, however, about how different types of RGCs target specific brain regions. Here we identify a guidance cue signaling pathway that is critical for the establishment of neural connectivity between retinal ganglion cells involved in the perception of self motion and

their central targets in the accessory optic system (AOS). We found that the transmembrane protein Sema6A is an On DSGC marker and is required for On DSGC-MTN innervation *in vivo*. PlexA2 and PlexA4, expressed by cells in the MTN, serve as ligands and signal through receptor Sema6A to attract On DSGC axon connections with the MTN. The connectivity mediated by PlexA2/A4-Sema6A reverse signaling facilitates the vertical OKR, a critical AOS function (Figure 8).

The establishment of RGC-central brain target connectivity relies on a series of developmental events that include initial retinorecipient targeting and further refinement of these connections (Haupt and Huber, 2008). DSGC axons that target the MTN extend either via the inferior (upward-preferring) or the superior (downward-preferring) fasciculi of the accessory optic tract, and therefore these two DSGC types must respond to distinct environmental cues to ultimately establish connections with specific MTN regions. In *Sema6A*$^{-/-}$ mutants, SPIG1::GFP^{+} On DSGC axons arrive in the vicinity of their target during mid-embryogenesis, however they exhibit a much broader innervation pattern compared to controls. These results show that Sema6A is essential at a relatively late step for mediating On DSGC target recognition, after other guidance molecules have guided On DSGC axons along their trajectories to this select midbrain region during early embryogenesis. Loss of Sema6A results in observable declines in MTN-innervating RGC cell numbers several days after the onset of RGC-MTN innervation defects. Thus, On DSGC cell loss is likely a secondary consequence of the On DSGC-MTN innervation phenotype. It remains to be determined whether or not Sema6A-PlexinA2/A4 signaling provides a pro-survival signal to On DSGCs that innervate the MTN.

We previously showed that Sema6A is a repellent cue that functions exclusively through the PlexA2 receptor to regulate SAC dendritic stratification and arborization (Sun et al., 2013). However, here we find that global deletion of *PlexA2*, and also select loss of *PlexA2* in the retina, does not affect DSGC-MTN innervation. This shows that that PlexA2 expressed by SACs is not required for Sema6A-mediated On DSGC-MTN innervation, and it also suggests that distinct ligand-receptor combinations are utilized to achieve functional connectivity in distinct DS circuits. We observed that PlexA2 and another Sema6A binding partner, PlexA4, function together, most likely in redundant fashion, to direct AOS retinorecipient targeting, providing additional evidence that plexin receptors act in concert to regulate semaphorin-dependent visual system development (Matsuoka et al., 2011a).

Transmembrane semaphorins, which were originally identified as ligands, can function as receptors and mediate “reverse signaling”. For example, the *Drosophila* transmembrane semaphorin 1a (Sema-1a) serves as a receptor during olfactory circuit assembly (Komiyama et al., 2007; Sweeney et al., 2011), visual system development (Cafferty et al., 2006; Yu et al., 2010) and motor axon pathfinding (Jeong et al., 2012). In vertebrates, semaphorin 6D (Sema6D) functions as a receptor for PlexA1 and regulates myocardial patterning during cardiac development (Toyofuku et al., 2004). Sema6A is also expressed by LGN neurons and is required for the elaboration of thalamocortical connectivity (Leighton et al., 2001; Little et al., 2009), suggesting that vertebrate transmembrane semaphorins also function as receptors during nervous system development. This idea receives support from a recent study showing that Sema6B functions as an axon guidance receptor in chick spinal cord

commissural axons for floor plate-derived PlexA2 (Andermatt et al., 2014). In our present study, we demonstrate that Sema6A is expressed in the On DSGCs that innervate the MTN, whereas PlexA2 and A4 are expressed by their target cells in the MTN and not in any RGCs. *In vitro*, On DSGC axons extending from SPIG1::GFP$^+$ RGCs preferentially extend along PlexA2- or PlexA4-coated surfaces, and this attractive response is dependent upon Sema6A expression in these DSGCs. Our expression analyses, loss-of-function genetic analyses *in vivo*, and *in vitro* RGC axon guidance assays strongly suggest that PlexA2/A4 expressed by cells of the MTN function as attractive cues to facilitate retinorecipient targeting of Sema6A$^+$ On DSGCs. These observations provide strong *in vivo* support for "reverse signaling" by transmembrane semaphorins in the vertebrate nervous system, with plexins serving as attractive ligands. PlexA2/A4-Sema6A reverse signaling during AOS circuit assembly may also provide a platform to investigate the underlying signaling mechanisms utilized by transmembrane semaphorins to regulate neural development.

We find that Sema6A is expressed by On DSGCs, but not by TRHR-GFP$^+$, DRD4-GFP$^+$ or CART$^+$ On-Off DSGCs. This restricted Sema6A expression is consistent with our observation that Sema6A is not required for retinorecipient targeting by subsets of On-Off DSGCs, and that Sema6A is also not required for the survival of most On-Off DSGC cells. Thus, functionally related retinal ganglion cells, in this case On DSGCs and On-Off DSGCs, have unique protein expression profiles allowing them to employ distinct molecular mechanisms to achieve correct retinorecipient targeting. This is underscored by our observations here of various RGC populations in the *Sema6A*$^{-/-}$ mutant background, revealing that the retinorecipient targeting to many, if not all, main optic system brain targets remains unchanged in *Sema6A*$^{-/-}$ mutants. These results show that the AOS utilizes a select cohort of molecules to direct retinorecipient innervation, perhaps reflecting the distinct origins and unique circuitry that define the AOS.

In addition to MTN targeting defects, we find that *PlexA2*$^{-/-}$*; PlexA4*$^{-/-}$ double mutants exhibit highly penetrant RGC-DTN targeting phenotypes. Furthermore, the hOKR, a visual behavior mediated by On DSGC-DTN/NOT innervation, is almost completely compromised in these double mutants. These hOKR deficits are in contrast to *Sema6A*$^{-/-}$ mutants, in which the RGC-DTN innervation and horizontal OKRs are much less affected. Therefore, we propose that other guidance cue receptors likely function along with Sema6A to mediate PlexA2/A4-dependent RGC-DTN targeting. In this regard it is interesting to note that an accompanying paper (Osterhout et al., 2015) shows that the immunoglobulin (Ig) superfamily member contactin-4 (CNTN4) and the amyloid precursor protein (APP) together are required in On DSGC for innervation of the NOT but not innervation of the MTN. These proteins function to regulate the arborization of On DSGC axons within the NOT, and loss of CNTN4 or APP results in OKR defects. It will be interesting to determine the complete array of guidance cues required for functional AOS connectivity, and the degree to which they independently or together regulate RGC axon target selection and arborization.

Our observations showing that PlexA2/A4-Sema6A signaling controls critical aspects of AOS development and function provide insight into the molecular mechanisms governing AOS circuit assembly between the retina and midbrain nuclei. Further, they provide a

foundation for describing unique AOS RGC subtypes. Future work will determine whether similar molecular machinery facilitates retinorecipient targeting by other RGC classes, and whether non-visual system neuronal cell types in the CNS also employ similar targeting mechanisms.

EXPERIMENTAL PROCEDURES

Animals

The day of vaginal plug observation was designated embryonic day 0.5 (e0.5), and the day of birth in this study was designated postnatal day 0 (P0). *Semaphorin 6A*$^{-/-}$ (*Sema6A*$^{-/-}$), *plexin A1*$^{-/-}$(*PlexA1*$^{-/-}$), *plexin A2*$^{-/-}$ (*PlexA2*$^{-/-}$), *plexin A3*$^{-/-}$ (*PlexA3*$^{-/-}$), *plexin A4*$^{-/-}$ (*PlexA4*$^{-/-}$), *plexin A2* ^{f} (*PlexA2*^{f}), *neuropilin1*^{f} (*Nrp1*^{f}), *neuropilin 2*$^{-/-}$ (*Nrp2*$^{-/-}$), and *Six3-Cre* mouse lines were described previously (Sun et al., 2013). The GFP knock-in line *SPIG1::GFP* and GFP BAC transgenic lines (*Hoxd10-GFP*, *TRHR-GFP*, *DRD4-GFP*, *CB2-GFP*, and *Cdh3-GFP*) were described previously (Dhande et al., 2013; Huberman et al., 2008b; Huberman et al., 2009; Kay et al., 2011; Osterhout et al., 2011; Rivlin-Etzion et al., 2011; Yonehara et al., 2009; Yonehara et al., 2008). The *Sox2-Cre* mouse line (stock number: 004783) and *ROSA*$^{LacZ/+}$ reporter mouse line (stock number: 003309) were obtained from the Jackson Laboratory.

Immunohistochemistry

Primary antibodies used in this study include: goat-anti-mouse Sema6A (R&D systems, 1:200), rabbit anti-GFP (Life Technologies, IgG fraction, 1:1000), rabbit anti-GFP (Life Technologies, serum, 1:1000), chicken anti-GFP (AVES, 1:1000), rabbit anti-CART (Phoenix Pharmaceuticals Inc., 1:1000), goat anti-ChAT (Millipore, 1:200), TO-PRO3 (Life Technologies, 1:500), rabbit anti-cleaved Caspase 3(Asp 175) (5A1E) (Cell Signaling Technology, 1:200), rabbit anti-Brn3b (gift from Dr. Jeremy Nathans, 1:200), rabbit anti-plexinA2 (gift from Dr. Fumikazu Suto, 1:200), Armenian hamster anti-plexinA4 (gift from Dr. Fumikazu Suto, 1:200), and mouse anti-TujIII (Promega, 1:1000).

Wholemount Retina Staining

Wholemount retina ICC was performed as previously described (Sun et al., 2013).

Cholera Toxin Subunit B (CTB) Injection

Bilateral CTB injection was performed as previously described (Riccomagno et al., 2014). Briefly, the adult animals were anesthetized using isophorone and then injected with 2 μL CTB-Alexa-555 or CTB-Alexa-488 (Life Technologies, 1mg/mL) bilaterally into the vitreous of each eye.

Stripe Assay

The axon guidance stripe assay was performed as previously described (Sun et al., 2013).

Optokinetic Reflex (OKR) Measurement

The OKR apparatus and recording methodology are as previously described (Cahill and Nathans, 2008).

Supplementary Material

Refer to Web version on PubMed Central for supplementary material.

ACKNOWLEDGEMENTS

We thank Drs. Samer Hattar, Rebecca James and Bredan Lilley for helpful comments on the manuscript. We also thank Marley Jamason for analysis of whole-mount RGC projections, Dontais Johnson for technical assistance, and members of Kolodkin laboratory for assistance and discussions. This work was supported by NIH RO1 EY022157-01 and a Pew Scholar Award (A.D.H.); A.L.K. and J.N. are investigators of the Howard Hughes Medical Institute.

REFERENCES

Andermatt I, Wilson NH, Bergmann T, Mauti O, Gesemann M, Sockanathan S, Stoeckli ET. Semaphorin 6B acts as a receptor in post-crossing commissural axon guidance. Development. 2014; 141:3709–3720. [PubMed: 25209245]

Badea TC, Cahill H, Ecker J, Hattar S, Nathans J. Distinct roles of transcription factors brn3a and brn3b in controlling the development, morphology, and function of retinal ganglion cells. Neuron. 2009; 61:852–864. [PubMed: 19323995]

Cafferty P, Yu L, Long H, Rao Y. Semaphorin-1a functions as a guidance receptor in the Drosophila visual system. The Journal of neuroscience : the official journal of the Society for Neuroscience. 2006; 26:3999–4003. [PubMed: 16611816]

Cahill H, Nathans J. The optokinetic reflex as a tool for quantitative analyses of nervous system function in mice: application to genetic and drug-induced variation. PloS one. 2008; 3:e2055. [PubMed: 18446207]

Culican SM, Bloom AJ, Weiner JA, DiAntonio A. Phr1 regulates retinogeniculate targeting independent of activity and ephrin-A signalling. Molecular and cellular neurosciences. 2009; 41:304–312. [PubMed: 19371781]

Dhande OS, Estevez ME, Quattrochi LE, El-Danaf RN, Nguyen PL, Berson DM, Huberman AD. Genetic dissection of retinal inputs to brainstem nuclei controlling image stabilization. The Journal of neuroscience : the official journal of the Society for Neuroscience. 2013; 33:17797–17813. [PubMed: 24198370]

Dhande OS, Huberman AD. Retinal ganglion cell maps in the brain: implications for visual processing. Current opinion in neurobiology. 2014; 24:133–142. [PubMed: 24492089]

Fredericks CA, Giolli RA, Blanks RH, Sadun AA. The human accessory optic system. Brain research. 1988; 454:116–122. [PubMed: 3408998]

Furuta Y, Lagutin O, Hogan BL, Oliver GC. Retina- and ventral forebrain-specific Cre recombinase activity in transgenic mice. Genesis. 2000; 26:130–132. [PubMed: 10686607]

Haupt C, Huber AB. How axons see their way--axonal guidance in the visual system. Frontiers in bioscience : a journal and virtual library. 2008; 13:3136–3149. [PubMed: 17981783]

Huberman AD, Feller MB, Chapman B. Mechanisms underlying development of visual maps and receptive fields. Annual review of neuroscience. 2008a; 31:479–509.

Huberman AD, Manu M, Koch SM, Susman MW, Lutz AB, Ullian EM, Baccus SA, Barres BA. Architecture and activity-mediated refinement of axonal projections from a mosaic of genetically identified retinal ganglion cells. Neuron. 2008b; 59:425–438. [PubMed: 18701068]

Huberman AD, Wei W, Elstrott J, Stafford BK, Feller MB, Barres BA. Genetic identification of an On-Off direction-selective retinal ganglion cell subtype reveals a layer-specific subcortical map of posterior motion. Neuron. 2009; 62:327–334. [PubMed: 19447089]

Jeong S, Juhaszova K, Kolodkin AL. The Control of semaphorin-1a–mediated reverse signaling by opposing pebble and RhoGAPp190 functions in drosophila. Neuron. 2012; 76:721–734. [PubMed: 23177958]

Kay JN, De la Huerta I, Kim IJ, Zhang Y, Yamagata M, Chu MW, Meister M, Sanes JR. Retinal ganglion cells with distinct directional preferences differ in molecular identity, structure, and central projections. The Journal of neuroscience : the official journal of the Society for Neuroscience. 2011; 31:7753–7762. [PubMed: 21613488]

Komiyama T, Sweeney LB, Schuldiner O, Garcia KC, Luo L. Graded expression of semaphorin-1a cell-autonomously directs dendritic targeting of olfactory projection neurons. Cell. 2007; 128:399–410. [PubMed: 17254975]

Kubo F, Hablitzel B, Dal Maschio M, Driever W, Baier H, Arrenberg AB. Functional architecture of an optic flow-responsive area that drives horizontal eye movements in zebrafish. Neuron. 2014; 81:1344–1359. [PubMed: 24656253]

Leighton PA, Mitchell KJ, Goodrich LV, Lu X, Pinson K, Scherz P, Skarnes WC, Tessier-Lavigne M. Defining brain wiring patterns and mechanisms through gene trapping in mice. Nature. 2001; 410:174–179. [PubMed: 11242070]

Little GE, Lopez-Bendito G, Runker AE, Garcia N, Pinon MC, Chedotal A, Molnar Z, Mitchell KJ. Specificity and plasticity of thalamocortical connections in Sema6A mutant mice. PLoS biology. 2009; 7:e98. [PubMed: 19402755]

Masseck OA, Hoffmann KP. Comparative neurobiology of the optokinetic reflex. Annals of the New York Academy of Sciences. 2009; 1164:430–439. [PubMed: 19645943]

Matsuoka RL, Chivatakarn O, Badea TC, Samuels IS, Cahill H, Katayama K, Kumar SR, Suto F, Chedotal A, Peachey NS, et al. Class 5 transmembrane semaphorins control selective Mammalian retinal lamination and function. Neuron. 2011a; 71:460–473. [PubMed: 21835343]

Matsuoka RL, Nguyen-Ba-Charvet KT, Parray A, Badea TC, Chedotal A, Kolodkin AL. Transmembrane semaphorin signalling controls laminar stratification in the mammalian retina. Nature. 2011b; 470:259–263. [PubMed: 21270798]

McLaughlin T, O'Leary DD. Molecular gradients and development of retinotopic maps. Annual review of neuroscience. 2005; 28:327–355.

Nie D, Di Nardo A, Han JM, Baharanyi H, Kramvis I, Huynh T, Dabora S, Codeluppi S, Pandolfi PP, Pasquale EB, et al. Tsc2-Rheb signaling regulates EphA-mediated axon guidance. Nat Neurosci. 2010; 13:163–172. [PubMed: 20062052]

Osterhout JA, El-Danaf RN, Nguyen PL, Huberman AD. Birthdate and outgrowth timing predict cellular mechanisms of axon target matching in the developing visual pathway. Cell reports. 2014; 8:1006–1017. [PubMed: 25088424]

Osterhout JA, Josten N, Yamada J, Pan F, Wu SW, Nguyen PL, Panagiotakos G, Inoue YU, Egusa SF, Volgyi B, et al. Cadherin-6 mediates axon-target matching in a non-image-forming visual circuit. Neuron. 2011; 71:632–639. [PubMed: 21867880]

Pak MW, Giolli RA, Pinto LH, Mangini NJ, Gregory KM, Vanable JW Jr. Retinopretectal and accessory optic projections of normal mice and the OKN-defective mutant mice beige, beige-J, and pearl. The Journal of comparative neurology. 1987; 258:435–446. [PubMed: 3584547]

Pequignot MO, Provost AC, Salle S, Taupin P, Sainton KM, Marchant D, Martinou JC, Ameisen JC, Jais JP, Abitbol M. Major role of BAX in apoptosis during retinal development and in establishment of a functional postnatal retina. Developmental dynamics : an official publication of the American Association of Anatomists. 2003; 228:231–238. [PubMed: 14517994]

Renaud J, Kerjan G, Sumita I, Zagar Y, Georget V, Kim D, Fouquet C, Suda K, Sanbo M, Suto F, et al. Plexin-A2 and its ligand, Sema6A, control nucleus-centrosome coupling in migrating granule cells. Nat Neurosci. 2008; 11:440–449. [PubMed: 18327254]

Riccomagno MM, Sun LO, Brady CM, Alexandropoulos K, Seo S, Kurokawa M, Kolodkin AL. Cas adaptor proteins organize the retinal ganglion cell layer downstream of integrin signaling. Neuron. 2014; 81:779–786. [PubMed: 24559672]

Rivlin-Etzion M, Zhou K, Wei W, Elstrott J, Nguyen PL, Barres BA, Huberman AD, Feller MB. Transgenic mice reveal unexpected diversity of on-off direction-selective retinal ganglion cell

subtypes and brain structures involved in motion processing. The Journal of neuroscience : the official journal of the Society for Neuroscience. 2011; 31:8760–8769. [PubMed: 21677160]

Robles E, Baier H. Assembly of synaptic laminae by axon guidance molecules. Current opinion in neurobiology. 2012; 22:799–804. [PubMed: 22632825]

Runker AE, Little GE, Suto F, Fujisawa H, Mitchell KJ. Semaphorin-6A controls guidance of corticospinal tract axons at multiple choice points. Neural development. 2008; 3:34. [PubMed: 19063725]

Sanes JR, Zipursky SL. Design principles of insect and vertebrate visual systems. Neuron. 2010; 66:15–36. [PubMed: 20399726]

Schmitt AM, Shi J, Wolf AM, Lu CC, King LA, Zou Y. Wnt-Ryk signalling mediates medial-lateral retinotectal topographic mapping. Nature. 2006; 439:31–37. [PubMed: 16280981]

Simpson JI. The accessory optic system. Annual review of neuroscience. 1984; 7:13–41.

Sun LO, Jiang Z, Rivlin-Etzion M, Hand R, Brady CM, Matsuoka RL, Yau KW, Feller MB, Kolodkin AL. On and off retinal circuit assembly by divergent molecular mechanisms. Science. 2013; 342:1241974. [PubMed: 24179230]

Suto F, Tsuboi M, Kamiya H, Mizuno H, Kiyama Y, Komai S, Shimizu M, Sanbo M, Yagi T, Hiromi Y, et al. Interactions between plexin-A2, plexin-A4, and semaphorin 6A control lamina-restricted projection of hippocampal mossy fibers. Neuron. 2007; 53:535–547. [PubMed: 17296555]

Sweeney LB, Chou YH, Wu Z, Joo W, Komiyama T, Potter CJ, Kolodkin AL, Garcia KC, Luo L. Secreted semaphorins from degenerating larval ORN axons direct adult projection neuron dendrite targeting. Neuron. 2011; 72:734–747. [PubMed: 22153371]

Tawarayama H, Yoshida Y, Suto F, Mitchell KJ, Fujisawa H. Roles of semaphorin-6B and plexin-A2 in lamina-restricted projection of hippocampal mossy fibers. The Journal of neuroscience : the official journal of the Society for Neuroscience. 2010; 30:7049–7060. [PubMed: 20484647]

Thompson H, Camand O, Barker D, Erskine L. Slit proteins regulate distinct aspects of retinal ganglion cell axon guidance within dorsal and ventral retina. The Journal of neuroscience : the official journal of the Society for Neuroscience. 2006; 26:8082–8091. [PubMed: 16885222]

Toyofuku T, Zhang H, Kumanogoh A, Takegahara N, Yabuki M, Harada K, Hori M, Kikutani H. Guidance of myocardial patterning in cardiac development by Sema6D reverse signalling. Nature cell biology. 2004; 6:1204–1211.

Triplett JW, Wei W, Gonzalez C, Sweeney NT, Huberman AD, Feller MB, Feldheim DA. Dendritic and axonal targeting patterns of a genetically-specified class of retinal ganglion cells that participate in image-forming circuits. Neural development. 2014; 9:2. [PubMed: 24495295]

Yonehara K, Ishikane H, Sakuta H, Shintani T, Nakamura-Yonehara K, Kamiji NL, Usui S, Noda M. Identification of retinal ganglion cells and their projections involved in central transmission of information about upward and downward image motion. PloS one. 2009; 4:e4320. [PubMed: 19177171]

Yonehara K, Shintani T, Suzuki R, Sakuta H, Takeuchi Y, Nakamura-Yonehara K, Noda M. Expression of SPIG1 reveals development of a retinal ganglion cell subtype projecting to the medial terminal nucleus in the mouse. PloS one. 2008; 3:e1533. [PubMed: 18253481]

Yu L, Zhou Y, Cheng S, Rao Y. Plexin a-semaphorin-1a reverse signaling regulates photoreceptor axon guidance in Drosophila. The Journal of neuroscience : the official journal of the Society for Neuroscience. 2010; 30:12151–12156. [PubMed: 20826677]

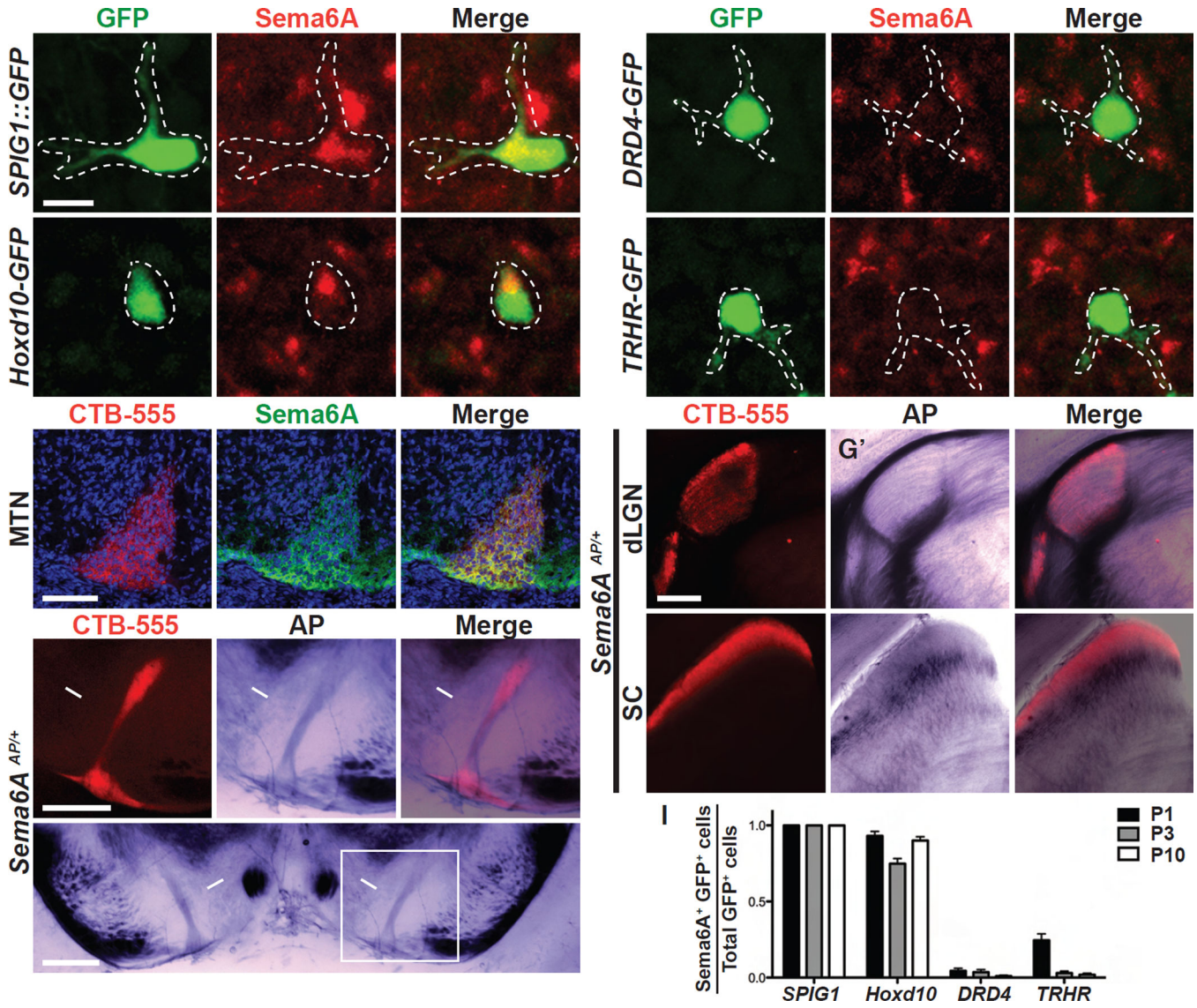

Figure 1. Sema6A is Expressed in On DSGCs but not *TRHR-GFP*$^+$ or *DRD4-GFP*$^+$ On-Off DSGCs

(A-B") Double immunostaining of *SPIG1::GFP*$^+$ (A-A") and *Hoxd10-GFP*$^+$ (B-B") RGCs by antibodies directed against GFP (green in A and B) and mouse Sema6A (red in A' and B'), showing that both *SPIG1::GFP*$^+$ and *Hoxd10-GFP*$^+$ cells express Sema6A (merged in A" and B", respectively). **(C-C")** Postnatal day 2 (P2) coronal brain sections showing that the axons innervating the medial terminal nucleus (MTN), labeled here by ocular injection of CTB-555 (C), are Sema6A immuno-positive (C' and C"). **(D-D"')** Colorimetric alkaline phosphatase (AP) enzymatic activity assay in adult *Sema6A* heterozygous mice (this line harbors a *Sema6A* AP "trap" allele and so expresses AP in Sema6A$^+$ tissues (Leighton et al., 2001)) reveals in coronal brain sections that retinal axons innervating the MTN (D, labeled by CTB-555 injection) express AP (D' and D"), providing additional evidence that Sema6A is expressed by On DSGCs that target to the MTN (n=7 animals). (D') is the enlarged view of the white inset in (D"'). **(E-F")** Double immunostaining of *DRD4-GFP*$^+$ (E-E") and

TRHR-GFP$^+$ (F-F") On-Off DSGCs with antibodies directed against GFP (E and F) and mouse Sema6A (E' and F'), showing that Sema6A is not expressed by *DRD4-GFP*$^+$ or *TRHR-GFP*$^+$ cells (E" and F"). **(G-H")** RGC axon targeting to the dorsal lateral geniculate nucleus (dLGN, G) and the superior colliculus (SC, H) observed in coronal brain sections following labeling by ocular injection of CTB-555 and subsequent AP enzymatic reactions (G' and H'), showing that RGC axons innervating the dLGN "shell" region and the superficial region of SC are AP (G" and H"). **(I)** Quantification of the ratio of Sema6A and GFP double immuno-positive cells to total GFP$^+$ cells in *SPIG1::GFP*, *Hoxd10-GFP*, *DRD4-GFP*, and *TRHR-GFP* retinas throughout early-postnatal retinal development (n≥5 sample areas from 2–4 retinas of each genotype). For *SPIG1::GFP* retinas: 68 GFP$^+$ and Sema6A$^+$ cells/ 68 total cells at P1 (100%); 39/39 at P3 (100%); and 69/69 at P10 (100%). For *Hoxd10-GFP* retinas: 49/54 at P1 (90.74%); 96/127 at P3 (75.59%); and 123/137 at P10 (89.78%). For *DRD4-GFP* retinas: 9/215 at P1 (4.19%); 3/87 at P3 (3.45%); and 2/216 at P10 (0.93%). For *TRHR-GFP* retinas: 74/325 at P1 (22.77%); 7/213 at P3 (3.29%)l and 3/159 at P10 (1.89%). Error bars: SEM. Scale bars: 10 μm in (A) for (A)-(B") and (E)-(F"); 100 μm in (C) for (C)-(C"); 200 μm in (D) for (D)-(D"); 200 μm in (D"'); and 200 μm in (G) for (G)-(H").

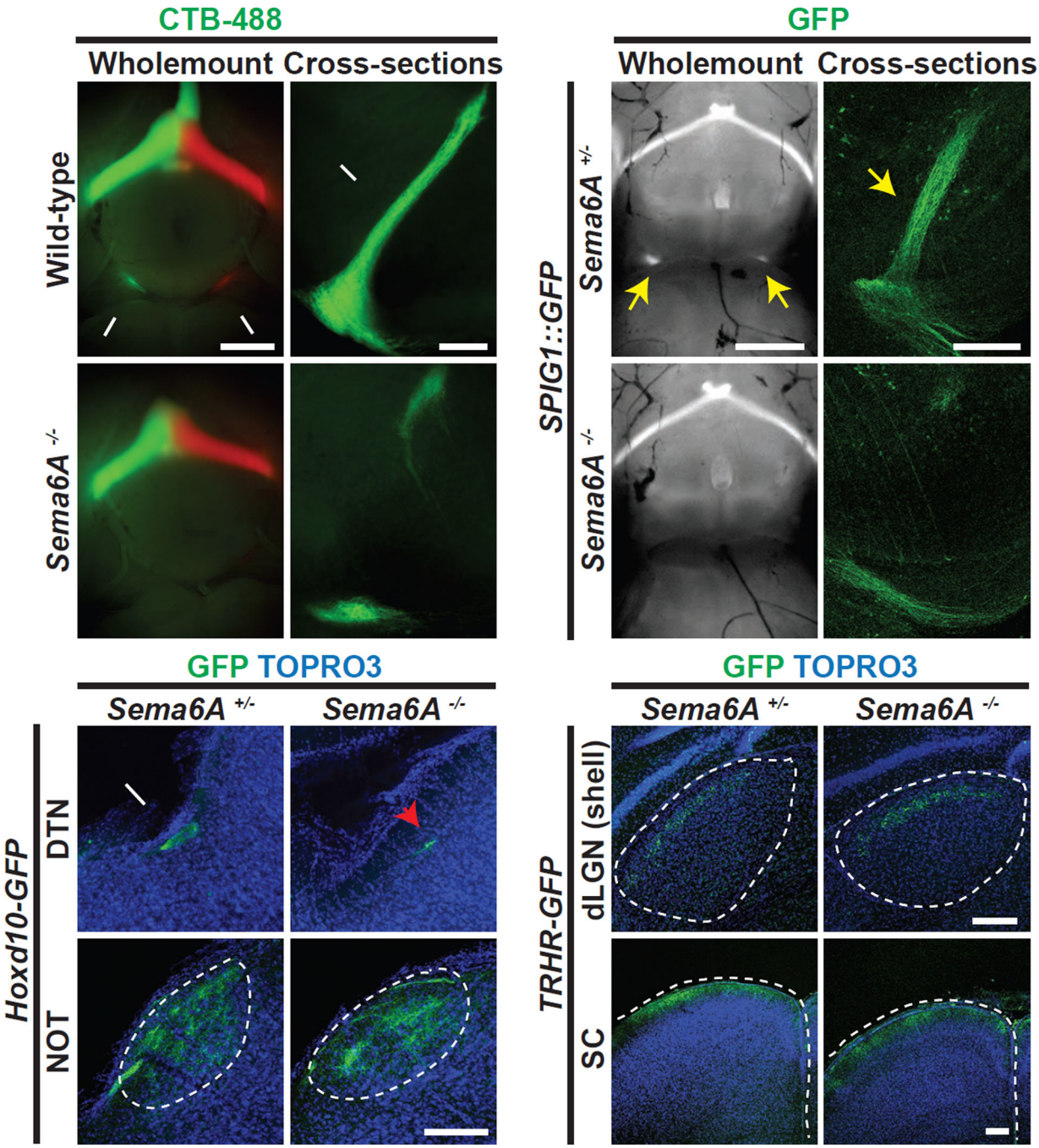

Figure 2. Sema6A is Required for the Development of Accessory Optic System Trajectories

(A and **B)** Wholemount ventral view (A) and cross-sectional view (B, higher magnification to reveal the MTN) of adult wild-type mouse brains with ocular injections of CTB-488 and CTB-555 bilaterally. Wild-type mice exhibit robust RGC-MTN innervation (white arrows in A and B) (n=7 wild-type mice). **(A'** and **B')** RGC-MTN innervation in *Sema6A*$^{-/-}$ mutants is greatly diminished, as observed in a ventral wholemount view (A') and a cross sectional view (B') (n=13 *Sema6A*$^{-/-}$ mutants, with phenotypes observed with full penetrance and expressivity). **(CD')** The On DSGC-MTN axon trajectory is illuminated by the *SPIG1::GFP*

reporter in *Sema6A*$^{+/-}$ (C and D) and *Sema6A*$^{-/-}$ brains (C' and D'). RGC-MTN innervation is prominent in P2 control animals (yellow arrows in C and D), whereas it is mostly abolished in *Sema6A*$^{-/-}$ mutants (C' and D') (n=3 animals for both genotypes). **(E-F')** Additional AOS trajectories are revealed by the *Hoxd10-GFP* reporter in *Sema6A*$^{+/-}$ (E and F) and *Sema6A*$^{-/-}$ mice (E' and F'). Compared to control (white arrow in E), dorsal terminal nucleus (DTN) innervation is reduced in *Sema6A*$^{-/-}$ mutants (red arrowhead in E'). Innervation of the nucleus of optic tract (NOT) is apparently preserved in *Sema6A*$^{-/-}$ mutants (compare F and F') (n≥4 animals for both genotypes). **(G-H')***TRHR-GFP*$^{+}$ On-Off DSGC axons project to the shell of dLGN (G) and the superficial layer of SC (H) in control animals. *Sema6A*$^{-/-}$ mutants (G' and H') exhibit similar innervation patterns compared to controls (G and H) (n=3 animals for both genotypes). Scale bars: 1mm in (A) for (A) and (A'); 200 μm in (B) for (B) and (B'); 1mm in (C) for (C) and (C'); 200 μm in (D) for (D) and (D'); 200 μm in (F') for (E)-(F'); 200 μm in (G') for (G) and (G'); and 200 μm in (H') for (H) and (H').

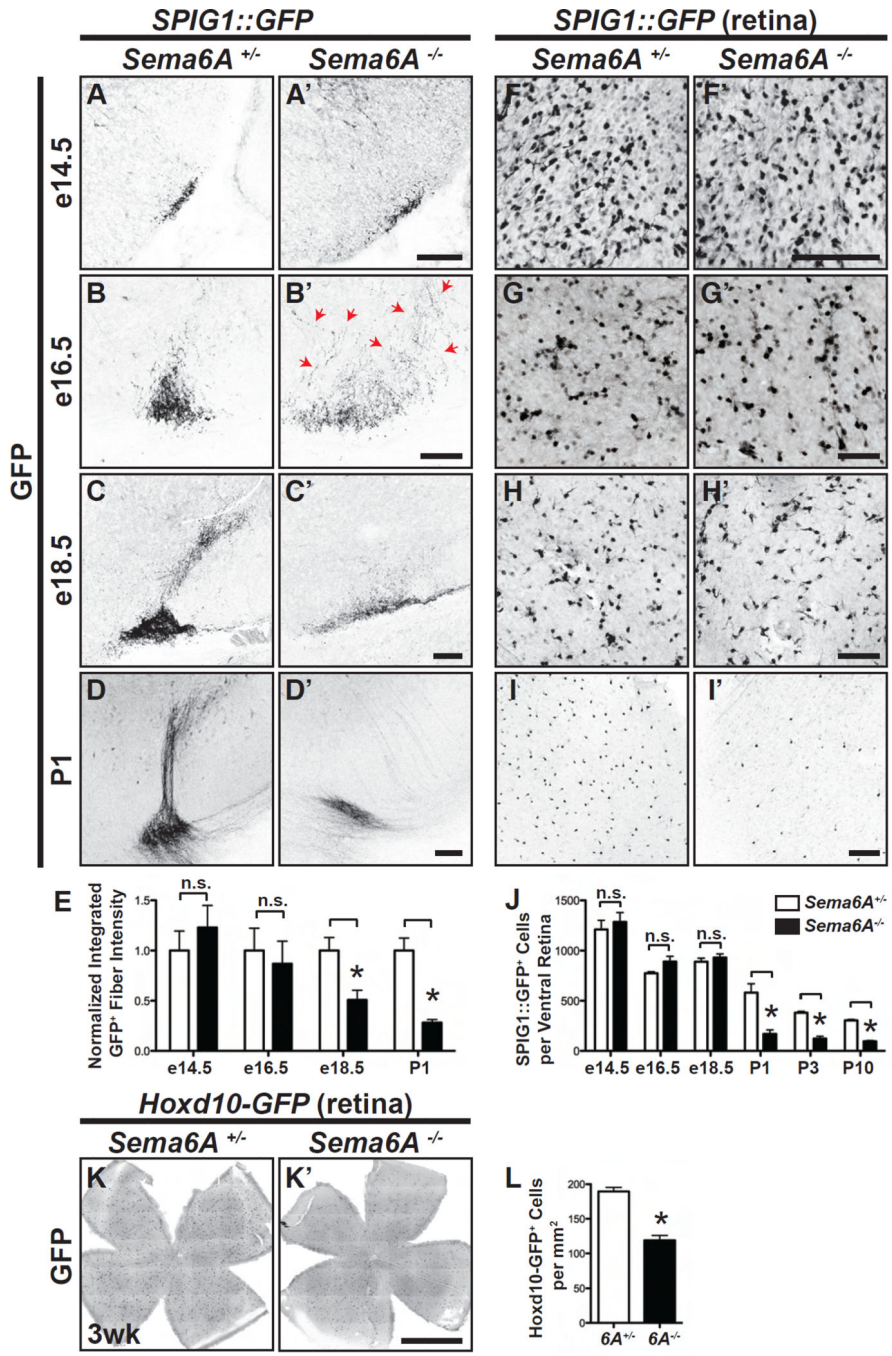

Figure 3. Developmental Characterization of On DSGC-MTN Innervation in *Sema6A*$^{-/-}$ Mutants

(A-D') On DSGC-MTN innervation revealed by *SPIG1::GFP* in *Sema6A*$^{+/-}$ (A–D) and *Sema6A*$^{-/-}$ animals (A'-D') throughout embryonic development. In control animals, SPIG1::GFP^{+} RGC axons arrive at the ventral MTN region as early as e14.5 (A), and the progression of MTN innervation is observed from e16.5 (B) to e18.5 (C). In *Sema6A*$^{-/-}$ mutants, On DSGC axons arrive at the target at e14.5 (A') and appear normal. However, by e16.5 these axons become defasciculated (red arrows in B'), and exhibit a much broader

innervation pattern in the region of the MTN compared to the control. These axons then begin to disappear throughout late embryonic development (C' and D'; quantification of innervation defects in Figure S3C; n≥3 animals for each developmental stage and for both genotypes analyzed). **(E)** Quantification of the normalized, integrated, GFP fluorescence to determine fiber density in controls and *Sema6A*$^{-/-}$ mutants. **(F-I')** Characterization of *SPIG1::GFP*$^{+}$ On DSGCs in the ventral region of *Sema6A*$^{+/-}$ (F–I) and *Sema6A*$^{-/-}$ (F'-I') retinas. No difference was observed between control and *Sema6A*$^{-/-}$ mutants at e16.5 or at e18.5 (compare G and G', H and H', and quantification in J). However, *Sema6A*$^{-/-}$ mutants (I') exhibit dramatically reduced numbers of GFP^{+} cells at P1 as compared to control (I) (n≥3 animals for each developmental stage and for both genotypes analyzed). **(J)** Quantification of *SPIG1::GFP*$^{+}$ cells in the ventral retina of *Sema6A*$^{+/-}$ and *Sema6A*$^{-/-}$ mice. **(K** and **K')** Representative images of a tile-scanned, flat-mounted, *Hoxd10-GFP; Sema6A*$^{+/-}$ retina (K) and a *Hoxd10-GFP; Sema6A*$^{-/-}$ retina (K'), showing that *Hoxd10-GFP; Sema6A*$^{-/-}$ retinas harbor fewer GFP^{+} RGCs. (**L**) Quantification of *Hoxd10-GFP*$^{+}$ cells in control and *Sema6A*$^{-/-}$ retinas (n=8 *Hoxd10-GFP; Sema6A*$^{+/-}$ retinas, and n=6 *Hoxd10-GFP; Sema6A*$^{-/-}$ retinas). Error bars: SEM. **P*<0.0001. Scale bars: 100 μm in (A)-(I'); and 1 mm in (K') for (K) and (K').

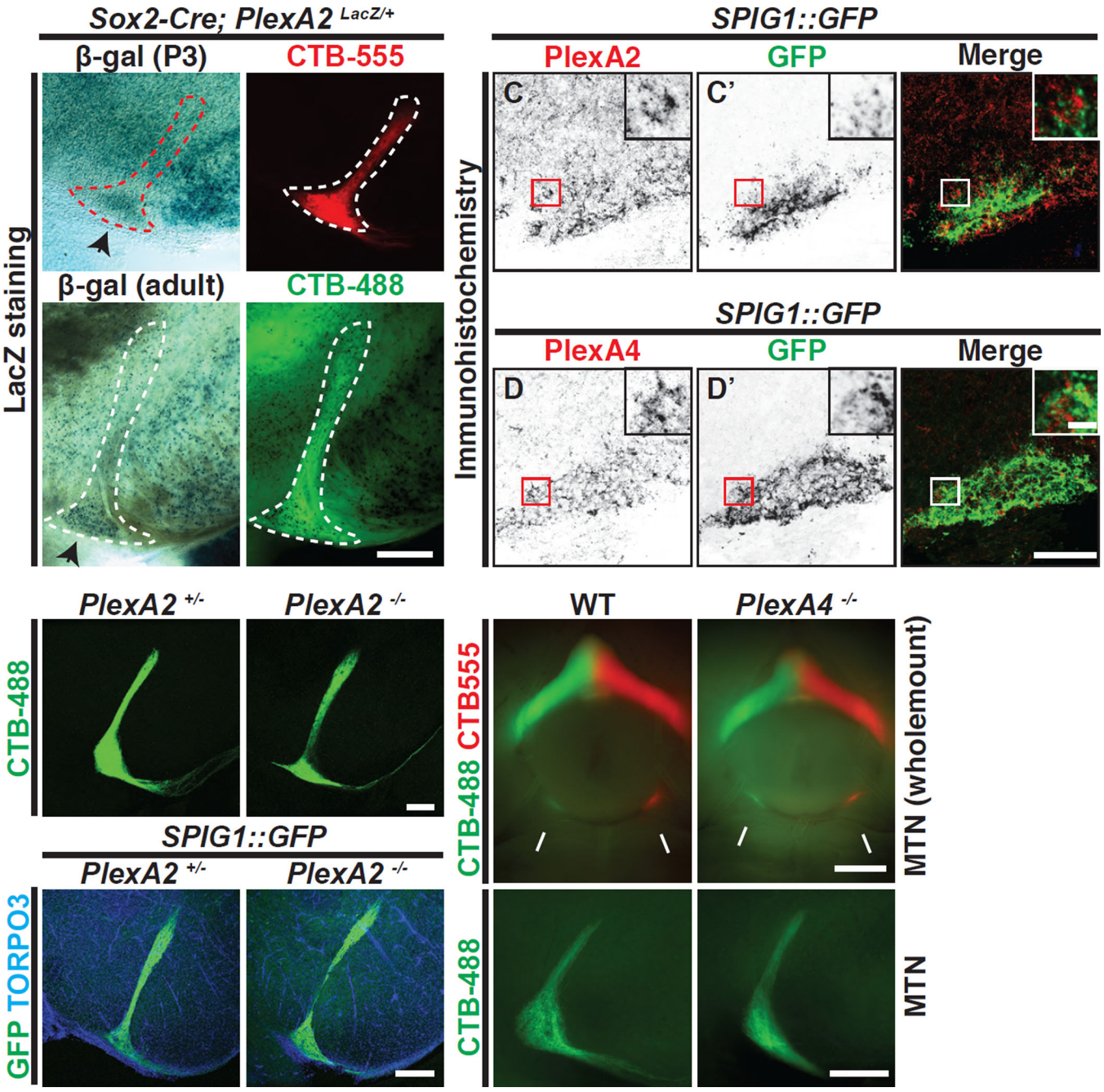

Figure 4. PlexA2 and A4 are Expressed in the MTN, and *PlexA2*$^{-/-}$ and *PlexA4*$^{-/-}$ Single Mutants Exhibit Normal On DSGC-MTN Innervation

(A-B') Expression of *PlexA2* in the MTN using ocular CTB injections (A' and B') and the *PlexA2* LacZ reporter encoded in the *PlexA2* conditional allele (Sun et al., 2013) (A and B), revealing that *PlexA2*$^{LacZ+}$ cells are abundant in the ventral region of the MTN at P3 and in the adult (black arrowheads in A and B, respectively; n=3 animals at each developmental stage). **(CD")** Immunostaining of PlexA2 (C) and PlexA4 proteins (D) in the MTN at e18.5 along with *SPIG1::GFP*$^{+}$ axon fibers to delineate the ventral MTN region (C' and D'). PlexA2 and PlexA4 proteins (C and D, respectively) are expressed in the MTN region, and

PlexA2^{+} and PlexA4^{+} cells (red boxes in C and D, respectively) are in very close proximity to *SPIG1::GFP*$^{+}$ fibers (red boxes in C' and D', and white boxes in C" and D"). **(E–H)** Characterization of RGC-MTN innervation in *PlexA2*$^{+/-}$ (E and G) and *PlexA2*$^{-/-}$ (F and H) animals by ocular CTB injections (E and F) and by genetic labeling (G and H). No obvious defects are observed in *PlexA2*$^{-/-}$ mutants (n=6 *PlexA2*$^{+/-}$ mice, n=8 *PlexA2*$^{-/-}$ mice; n=3 *SPIG1::GFP; PlexA2*$^{+/-}$ and 3 *SPIG1::GFP; PlexA2*$^{-/-}$ mice). **(I–L)** Wholemount ventral view (I and J) and cross-sectional view (K and L) of On-DSGC MTN innervation visualized by ocular CTB injections in WT (I and K) and *PlexA4*$^{-/-}$ mutants (J and L). On DSGC-MTN innervation appears normal in *PlexA4*$^{-/-}$ mutants (compare I and J, K and L; also see (Matsuoka et al., 2011b) Supplementary Figure 6) (n=4 WT; n=5 *PlexA4*$^{-/-}$ mutants). Scale bars: 250 μm in (B') for (A)-(B'); 100 μm in (D") for (C)-(D"); 10 μm in the inset of (D") for insets of (C)-(D"); 250 μm in (F) for (E) and (F); 250 μm in (H) for (G) and (H); 1 mm in (J) for (I) and (J); and 250 μm in (L) for (K) and (L).

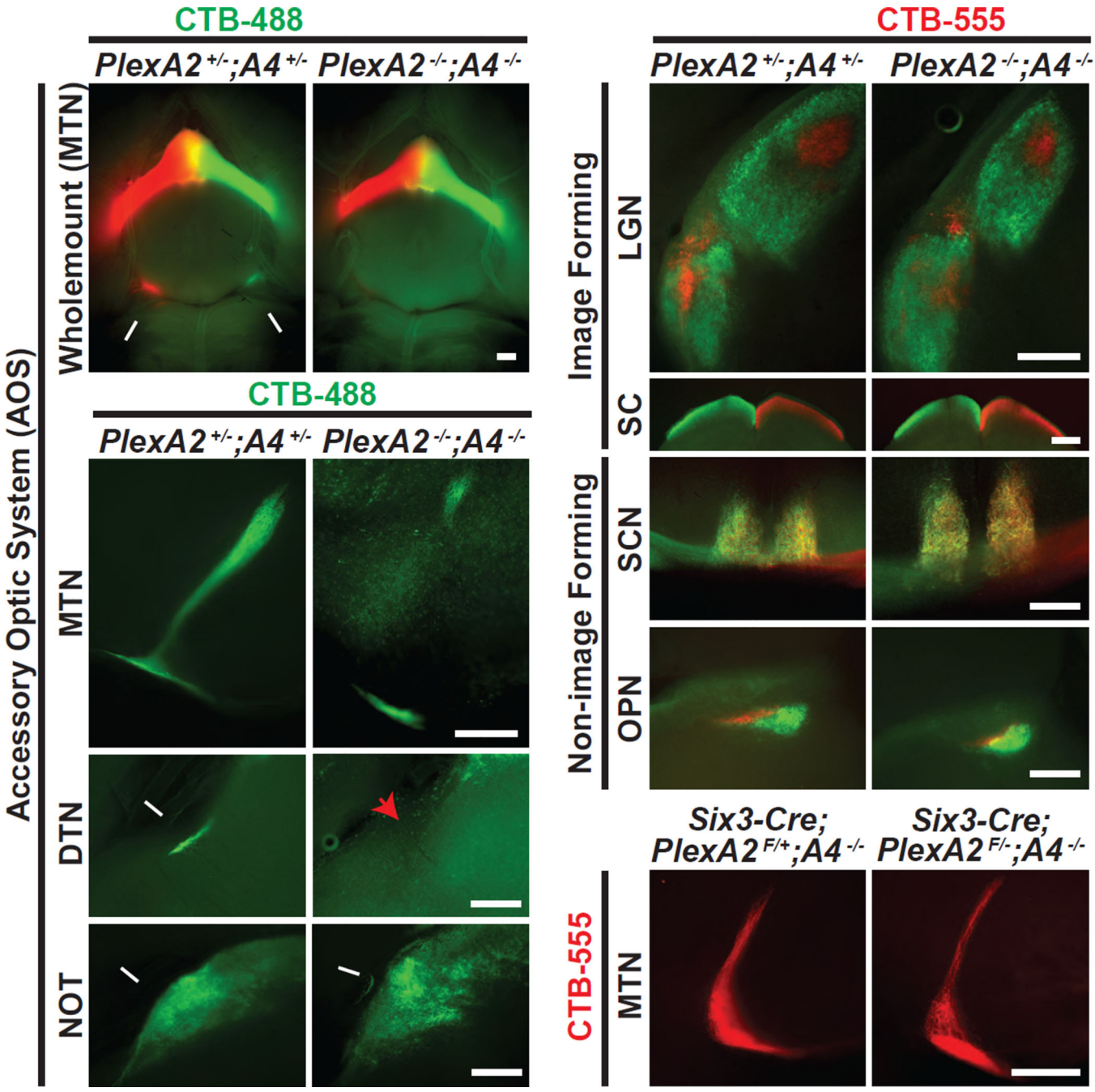

Figure 5. *PlexA2*$^{-/-}$;*PlexA4*$^{-/-}$ Double Mutants Phenocopy *Sema6A*$^{-/-}$ Single Mutants with Respect to On DSGC-MTN Innervation

(A and **A')** Ventral wholemount view of *PlexA2*$^{+/-}$;*PlexA4*$^{+/-}$ (A) and *PlexA2*$^{-/-}$;*PlexA4*$^{-/-}$ (A') adult brains following ocular injections with CTB-488 and CTB-555 bilaterally. Prominent projections to the MTN were observed in *PlexA2*$^{+/-}$;*PlexA4*$^{+/-}$ animals (white arrows in A), whereas MTN innervation is greatly diminished in *PlexA2*$^{-/-}$;*PlexA4*$^{-/-}$ mutants (A'), phenocopying *Sema6A*$^{-/-}$ mutants (n=9 *PlexA2*$^{+/-}$; *PlexA4*$^{+/-}$ mice; n=9 *PlexA2*$^{-/-}$; *PlexA4*$^{-/-}$ mutants, with 8/9 showing full expressivity). **(B-D')** Cross-sectional views of the accessory optic visual system in

PlexA2$^{+/-}$;*PlexA4*$^{+/-}$ (B–D) and *PlexA2*$^{-/-}$;*PlexA4*$^{-/-}$ (B'-D') mice. Compared to controls, *PlexA2*$^{-/-}$;*PlexA4*$^{-/-}$ mutants exhibit greatly reduced MTN innervation (B'), a complete loss of DTN innervation (red arrowhead in C'), but apparently normal NOT innervation (white arrow in D'). **(E-H')** Characterization of RGC axonal innervation to image-forming (E, E', F, F') and non-image-forming (G, G', H, H') retinorecipient targets in controls (E–H) and *PlexA2*$^{-/-}$;*PlexA4*$^{-/-}$ mutants (E'-H'). In comparison to controls, the segregation of ipsilateral and contralateral retinal projections and general retinorecipient targeting are preserved in *PlexA2*$^{-/-}$;*PlexA4*$^{-/-}$ mutants (n=9 *PlexA2*$^{+/-}$;*PlexA4*$^{+/-}$ mice; n=9 *PlexA2*$^{-/-}$;*PlexA4*$^{-/-}$ mutants). **(I** and **I')** Removal of *PlexA2* genetically in a *PlexA4*$^{-/-}$ mutant background (I') results in similar MTN innervation as in the control (I), showing that retina-derived PlexA2 is not required for normal development of On DSGC-MTN projections (n=4 animals for both genotypes). Scale bars: 250 μm.

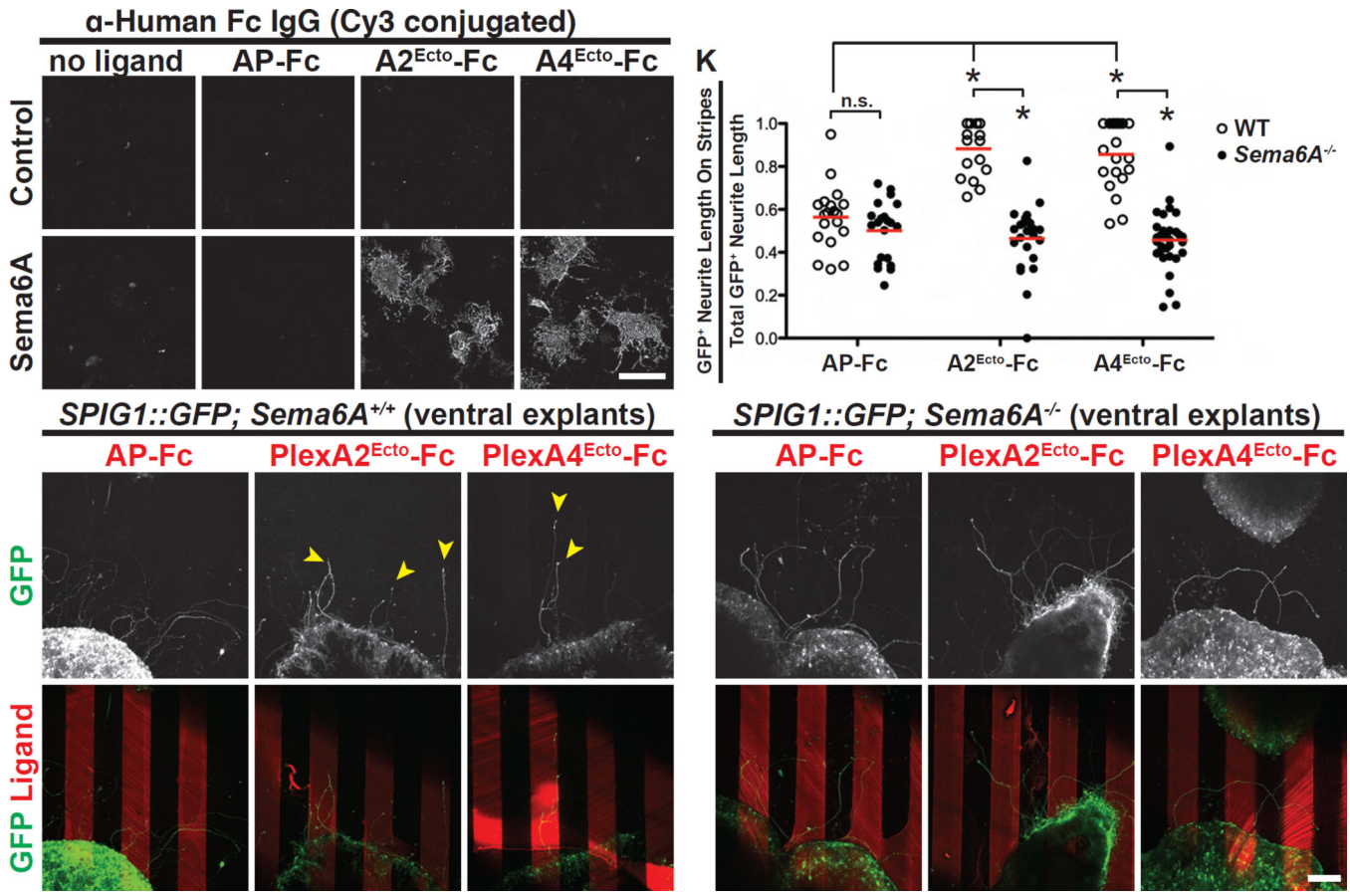

Figure 6. PlexA2 and A4 Function as Attractive Cues for *SPIG1::GFP*$^{+}$ On DSGC Neurites *in vitro*

(A-D') Fluorescent ligand binding assay showing that PlexA2 and PlexA4 ectodomain recombinant proteins only bind to COS7 cells that express mouse Sema6A *in vitro* (C' and D'). **(E-G')** The ventral region of *SPIG1::GFP; Sema6A*$^{+/+}$ retinas was dissected out and cultured on plates coated with recombinant proteins presented as "stripes" (Sun et al., 2013). After two days *in vitro*, SPIG1::GFP^{+} neurites that extended from explants show no preferences for AP-Fc stripes (E and E'). In contrast, SPIG1::GFP^{+} neurites preferentially grew on PlexA2^{Ecto}-Fc and PlexA4^{Ecto}-Fc recombinant protein stripes (yellow arrowheads in F and G, respectively) (n=19 explants on AP-Fc stripes, n=17 explants on PlexA2^{ecto}-Fc stripes, and n=21 explants on PlexA4^{ecto}-Fc stripes; the explants were from 9 embryos). **(H-J')** SPIG1::GFP^{+} neurites extending from *SPIG1::GFP; Sema6A*$^{-/-}$ ventral retina explants exhibit no preference for AP-Fc (H and H'), PlexA2^{Ecto}-Fc (I and I'), or PlexA4^{Ecto}-Fc stripes (J and J') (n=21 explants on AP-Fc stripes, n=24 explants on PlexA2^{Ecto}-Fc stripes, and n=35 explants on PlexA4^{Ecto}-Fc stripes; explants were from 9 embryos). **(K)** Quantification of GFP^{+} neurite length on stripes over the total GFP^{+} neurite length in the stripe assay. Red bars represent the mean for each group. *$P<10^{-6}$. Scale bars: 100 μm in (D') for (A)-(D'); and 100 μm in (J') for (E)-(J').

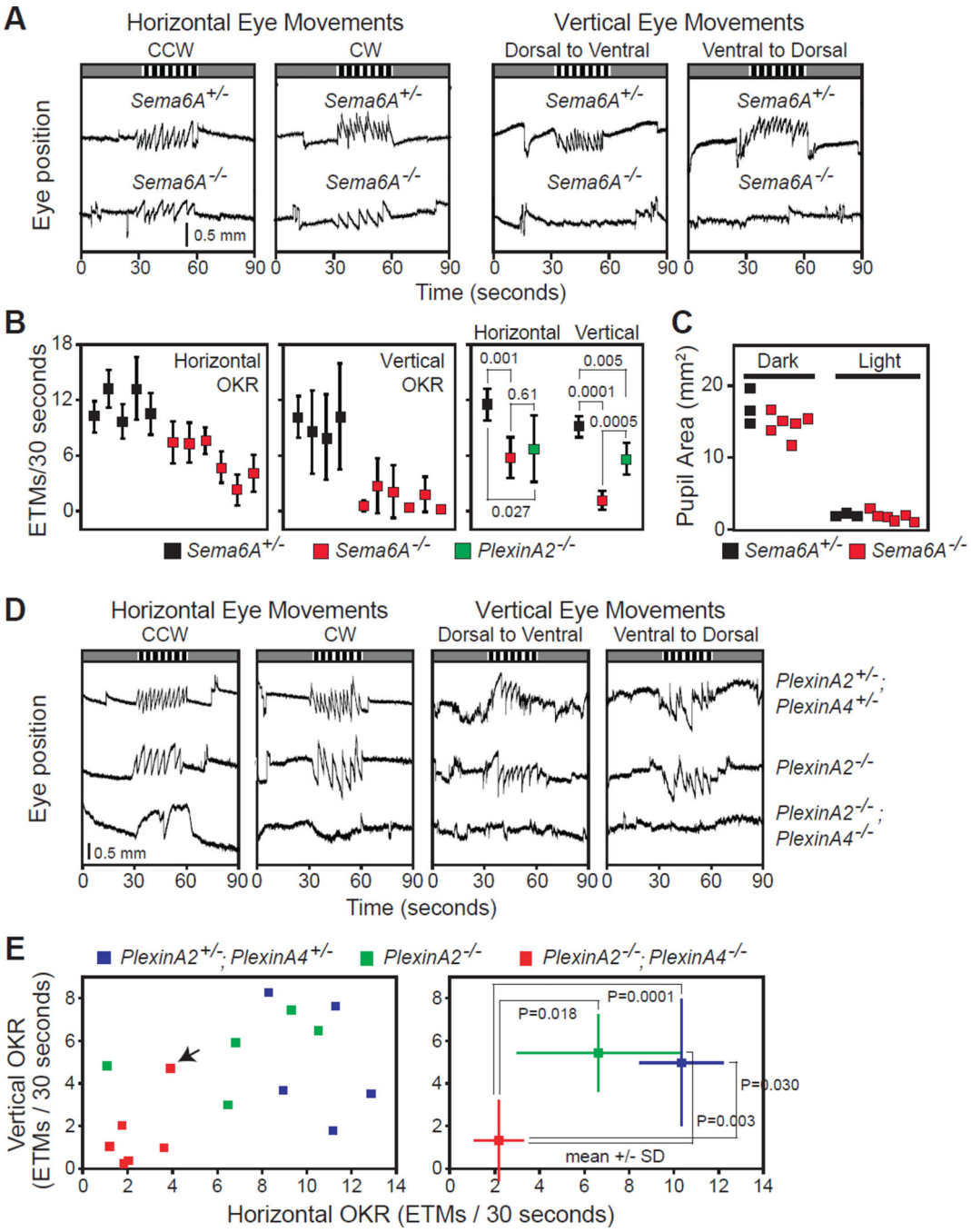

Figure 7. Loss of PlexA2/A4-Sema6A Signaling Compromises Optokinetic Reflex (OKR) Responses

(A) OKR of *Sema6A*$^{+/-}$ (top) and *Sema6A*$^{-/-}$ mice (bottom) measured by infrared imaging of eye position in response to horizontal (left two columns) or vertical (right two columns) motion of black and white stripes during a 30-second time interval (indicated by the striped pattern at the top of each panel). Prior to and following the stimulus interval there are two 30-second periods with no moving stimuli. Asymmetric saw-tooth eye tracking movements (ETMs) illuminate the OKR. *Sema6A*$^{-/-}$ mutants retain significant horizontal OKR

responses (left panel) but exhibit no vertical OKR (right two panels). **(B)** Quantification of the average number of eye tracking movements (each ETM is defined as a slow tracking movement followed by a rapid saccade) per 30-second interval. Left panel, horizontal OKR of *Sema6A*$^{+/-}$ and *Sema6A*$^{-/-}$ animals. Middle panel, vertical OKR in *Sema6A*$^{+/-}$ and *Sema6A*$^{-/-}$ animals. Right panel, quantification and comparison of hOKR and vOKR among *Sema6A*$^{+/-}$, *Sema6A*$^{-/-}$, and *PlexA2*$^{-/-}$ mice. **(C)** Pupil light reflex (PLR) test (measured by pupil area, mm^2) of *Sema6A*$^{+/-}$ and *Sema6A*$^{-/-}$ mice showing that *Sema6A*$^{-/-}$ mutants have normal PLR responses. **(D)** Representative horizontal OKR (left two columns) and vertical OKR (right two columns) responses in *PlexA2*$^{+/-}$*;PlexA4*$^{+/-}$ (upper row), *PlexA2*$^{-/-}$ (middle row), and *PlexA2*$^{-/-}$*;PlexA4*$^{-/-}$ animals (bottom row). *PlexA2*$^{-/-}$*;PlexA4*$^{-/-}$ animals exhibit loss of both horizontal and vertical OKR responses. **(E)** Quantification of the horizontal and vertical OKRs in *PlexA2*$^{+/-}$*;PlexA4*$^{+/-}$, *PlexA2*$^{-/-}$, and *PlexA2*$^{-/-}$*;PlexA4*$^{-/-}$ animals. Left panel, mean values for each mouse tested for OKR. The single *PlexA4*$^{-/-}$*;PlexA2*$^{-/-}$ mouse that showed significant vertical ETMs (mouse #8191, which shows limited MTN innervation (Figure S8H), is indicated by a black arrow). Right panel, mean±S.D. for each genotype; statistically significant *P* values are shown.

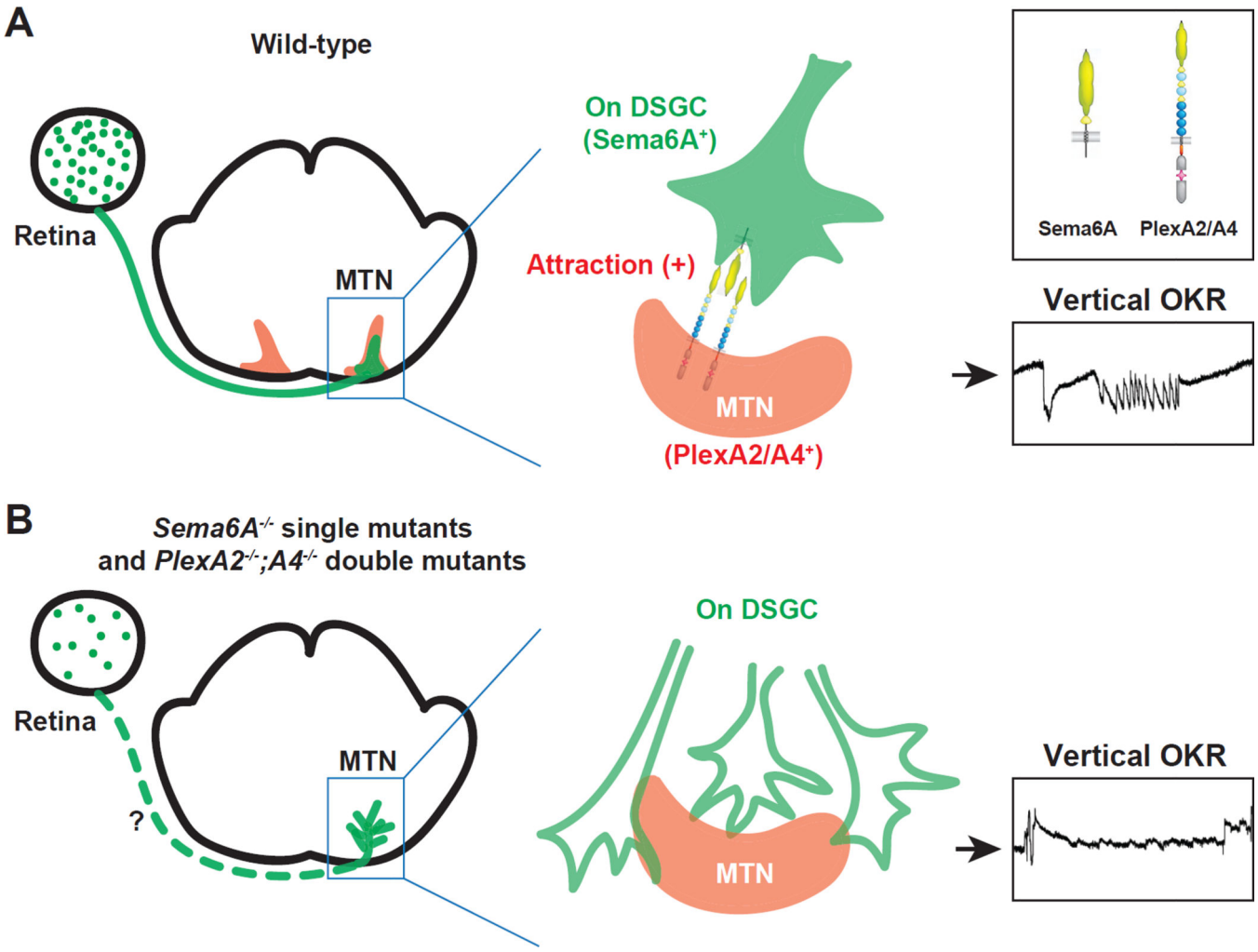

Figure 8. PlexA2/A4-Sema6A Signaling Guides the Functional Assembly of Mammalian Accessory Optic System Connections

(A) During late embryonic development, subsets of On DSGCs express the transmembrane protein Sema6A, arrive at the MTN target region and are attracted by cells in the MTN that express PlexA2 and PlexA4. PlexA2 and A4 serve as attractive ligands and signal through Sema6A to stabilize On DSGC-MTN innervation. Accurate connections between On DSGC axons and the MTN ensure correct assembly of AOS circuits critical for mediating the vertical OKR response. **(B)** In *Sema6A*$^{-/-}$ single mutants and *PlexA2*$^{-/-}$*;PlexA4*$^{-/-}$ double mutants, On DSGC axons fail to correctly target the MTN and subsequently exhibit cell loss in the retina, thereby resulting in diminished vertical OKR responses. In addition, *PlexA2*$^{-/-}$*;PlexA4*$^{-/-}$ double mutants show defects in RGC-DTN innervation, in line with the defective horizontal OKR responses observed in these double mutants (not shown).